ARMY RESEARCH LABORATORY

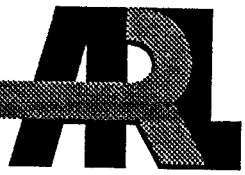

Terminal Ballistics of a Reduced-Mass Penetrator

Graham F. Silsby

ARL-MR-320

July 1996

REPORT DOCUMENTATION PAGE

Form Approved
OMB No. 0704-0188

1. AGENCY USE ONLY (Leave blank)	2. REPORT DATE	3. REPORT TYPE AND DATES COVERED
	July 1996	Final, Jan 90–Dec 95

4. TITLE AND SUBTITLE

Terminal Ballistics of a Reduced-Mass Penetrator

5. FUNDING NUMBERS

PR: 1L162618AH80

6. AUTHOR(S)

Graham F. Silsby

7. PERFORMING ORGANIZATION NAME(S) AND ADDRESS(ES)

U.S. Army Research Laboratory
ATTN: AMSRL-WT-TC
Aberdeen Proving Ground, MD 21005-5066

8. PERFORMING ORGANIZATION REPORT NUMBER

ARL-MR-320

9. SPONSORING/MONITORING AGENCY NAME(S) AND ADDRESS(ES)

10. SPONSORING/MONITORING AGENCY REPORT NUMBER

11. SUPPLEMENTARY NOTES

12a. DISTRIBUTION/AVAILABILITY STATEMENT

Approved for public release; distribution is unlimited.

12b. DISTRIBUTION CODE

13. ABSTRACT *(Maximum 200 words)*

This report presents the results of an experimental program to examine the performance of a reduced-mass concept penetrator impacting semi-infinite rolled homogeneous armor (RHA) at normal incidence. The reduced-mass penetrator used in this program is a solid tungsten alloy rod with eight holes drilled parallel to its axis, equally spaced on a circle, with axes parallel to the rod axis. Its performance was contrasted with baseline data for length-to-diameter ratios (*L/D*) 4 and 5 solid tungsten alloy penetrators. Striking velocity was nominally 1.6 km/s. A determined effort to reduce the scatter in the data by analysis of collateral data from the U.S. Army Research Laboratory (ARL) and literature sources suggested only a rather weak influence of *L/D* on penetration even at *L/D*s approaching 1 and provided a tentative relationship to remove the influence of target lateral edge effects. It tightened up the holed-out rod data enough to be able to conclude with a moderate degree of certainty that there was no improvement in penetration as suggested by a simplistic density law model. A companion work by Kimsey of ARL examines the performance of this novel penetrator concept computationally, using the Eulerian code CTH. His work explains the possible causes of reduced performance suggested by analysis by Zook and Frank of ARL, though with some relative improvement in performance at higher velocities.

14. SUBJECT TERMS

terminal ballistics, ballistics, penetrator, tungsten alloy, long rod penetrator

15. NUMBER OF PAGES

64

16. PRICE CODE

17. SECURITY CLASSIFICATION OF REPORT	18. SECURITY CLASSIFICATION OF THIS PAGE	19. SECURITY CLASSIFICATION OF ABSTRACT	20. LIMITATION OF ABSTRACT
UNCLASSIFIED	UNCLASSIFIED	UNCLASSIFIED	UL

INTENTIONALLY LEFT BLANK.

DISCLAIMER

ACKNOWLEDGMENTS

I would like to acknowledge the support of Dr. L. Puckett, the Associate Technical Director of the U.S. Army Ballistic Research Laboratory (BRL),* now of the Weapons Technology Directorate of the U.S. Army Research Laboratory (ARL), for suggesting the concept upon which this work is based and for his insightful discussions that guided the direction in which his concept was reduced to practice. I would like to thank Dr. W. de Rosset, Chief of the Penetration Mechanics Branch (PMB) of the Terminal Ballistics Division (TBD) for financial support that permitted the initial shots to be fired to determine concept feasibility. Dr. J. Frasier, the Director of the BRL, provided substantial funding for the main body of the work under the In-Laboratory Initiated Research program. The Armor Mechanics Branch (AMB) graciously provided the tungsten alloy rods used in the firings and permitted access to an extensive body of experimental data that expands the baseline against which the results of this program can be compared. Thanks also go to Dr. R. Shnidman of ARL's Survivability/Lethality Assessment Directorate, who very capably reviewed the draft of this report.

Discussions with others at the author's laboratory were very helpful. Konrad Frank and Todd Bjerke acted as sounding boards and provided very useful feedback. The work of Lori Pridgeon to characterize the effect of inadequate lateral target dimensions, currently underway, confirmed unequivocally a suspected source of uncontrolled variability in the data. When complete, her work will provide a rational means for workers to select a minimum lateral target dimension in terminal ballistic experiments, avoiding some of the problems which led to the need for extensive analysis of the data in this work. More such basic work needs to be done to reduce the costs of future programs and increase their credibility. Many other coworkers helped with advice on specific topics. Finally, I would like to acknowledge the substantial contributions of my associate Kent Kimsey, who collaborated in this effort, doing the finite difference modeling which has led to the understanding of the results. His advice and counsel are always on the mark.

* The U.S. Army Ballistic Research Laboratory (BRL) was deactivated on 30 September 1992 and subsequently became a part of the U.S. Army Research Laboratory (ARL) on 1 October 1992.

INTENTIONALLY LEFT BLANK.

TABLE OF CONTENTS

		Page
	ACKNOWLEDGMENTS	iii
	LIST OF FIGURES	vii
	LIST OF TABLES	ix
1.	BACKGROUND	1
2.	EXISTING DATA	3
3.	APPROACH	6
4.	EXPERIMENTAL RESULTS	7
5.	ANALYSIS	10
5.1	Yaw, Target Hardness Eliminated as a Source of Variability	11
5.2	Other Influences Sought	11
5.3	Inadequate Lateral Confinement, *L/D* Effects Suspected	13
5.4	Other Data Needed	14
5.5	*L/D* Effect Surprisingly Small for Long Rods	15
5.6	Lateral Constraint Effect Consistent With Recent Results of Others	18
5.7	Predicted Behavior for Large Targets	20
6.	INTERPRETATION	23
7.	TUBULAR PENETRATOR INSIGHTS	26
8.	CONCLUSIONS AND RECOMMENDATIONS	27
9.	REFERENCES	31
	APPENDIX A: HYPERVELOCITY PENETRATION DATABASE	33
	APPENDIX B: U.S. ARMY RESEARCH LABORATORY (ARL) RANGE 309A X21C ROLLED HOMOGENEOUS ARMOR (RHA) NORMAL-INCIDENCE PENETRATION DATABASE	39
	APPENDIX C: ANALYSIS DETAILS	49
	DISTRIBUTION LIST	57

INTENTIONALLY LEFT BLANK.

LIST OF FIGURES

Figure		Page
1.	Tungsten long rod vs. steel hypervelocity database and modified exponential fit (see Appendix A, Table A-1)	5
2.	Rod geometries	8
3.	Push-launch package design for 50-mm, smoothbore, high-pressure powder gun, Range 309A	8
4.	Penetration vs. velocity for various rod geometries	10
5.	Penetration normalized by rod length vs. velocity for the same data set	11
6.	Target (least) lateral web defined	14
7.	Raw *P/L* vs. *L/D* relationship	16
8.	*P/L* vs. *L/D* fit for $L/D > 0.01$, plotted on log-linear scale	17
9.	Scatter plots of residuals to multiple regression	19
10.	Increase in penetration with decrease in lateral confinement at 1,500 m/s	21
11.	Penetration data corrected for target lateral confinement	22
12.	Penetration of holed-out rod compared with baseline	23
13.	Numerical predictions compared with corrected data	25
14.	Confidence intervals around straight-line fit to holed-out rod data	28
C-1.	Individual fits to data of Farrand fit by multiple regression	55

INTENTIONALLY LEFT BLANK.

LIST OF TABLES

Table		Page
1.	Corrected Fit to Data Compared With Tate-Alekseevskii Predictions of Zook and Frank. Velocity is 1.6 km/s	24
2.	Projected Solid Rod RHA Unit Penetration	29
A-1.	Database and Notes	35
B-1.	Data Tabulation and Notes	41
B-2.	Detailed Explanation of Database Format	46
C-1.	Pooled Data Set of R309A and Farrand, With Notes	51
C-2.	Fitting Parameters for Individual and Multiple Regression	54

INTENTIONALLY LEFT BLANK.

1. BACKGROUND

Dr. Puckett conceived of a novel kinetic energy penetrator geometry that simple theory suggests would promise increased penetration at higher striking velocities. Conceptually, a long rod penetrator is lengthened and the excess mass so added is then removed by drilling out a pattern of holes parallel to the axis near the periphery through the entire length of the rod, decreasing its apparent density. If the density law holds, the increase in penetration due to increased length should more than offset the loss of penetration due to the decrease in apparent rod density.

The density law is derived from simple physical principles and the assumption that the striking velocity is high enough that inertial forces greatly exceed penetrator and material strength values. Follow the derivation below to see the interplay of the effects of length and density that suggest that a longer, lower density rod of the same diameter and mass should outperform a higher density one.

Define ρ as material density, P as an increment of target penetration, and L as the increment of penetrator length eroded to cause that target penetration. Use p and t as subscripts for penetrator and target, respectively, and use 1 and 2 as subscripts to identify two specific, different penetrator materials. Consider the mass balance on two streams of strengthless fluids of equal area impacting each other coaxially. In a frame of reference fixed relative to the interface between the two streams, assume that the two streams of fluid exit the impact zone radially. Solve the momentum equation for the relative velocities, and translate back to a frame of reference fixed relative to the "target" stream. This yields the well-known density law, which relates the relative erosion rates of penetrator and target to the material densities,

$$\frac{P}{L} = \sqrt{\frac{\rho_p}{\rho_t}}. \qquad (1)$$

Then,

$$\frac{\frac{P_2}{L_2}}{\frac{P_1}{L_1}} = \frac{\sqrt{\frac{\rho_{p2}}{\rho_t}}}{\sqrt{\frac{\rho_{p1}}{\rho_t}}}, \tag{2}$$

or,

$$\frac{P_2}{P_1} = \frac{L_2}{L_1}\frac{\sqrt{\rho_{p2}}}{\sqrt{\rho_{p1}}} = \frac{L_2}{L_1}\sqrt{\frac{\rho_{p2}}{\rho_{p1}}}. \tag{3}$$

For two right circular cylindrical streams of equal diameters, the lengths having equal masses are in inverse proportion to their densities,

$$\frac{L_1}{L_2} = \frac{\frac{4\,m}{\pi\,D^2\,\rho_{p1}}}{\frac{4\,m}{\pi\,D^2\,\rho_{p2}}} = \frac{\rho_{p2}}{\rho_{p1}}. \tag{4}$$

Substituting Equation 4 into 3 describes how a target material is penetrated by incremental lengths of penetrator streams of equal areas but different densities, on a penetrator stream mass-for-mass basis:

$$\frac{P_2}{P_1} = \frac{\rho_{p_1}}{\rho_{p2}}\frac{\sqrt{\rho_{p2}}}{\sqrt{\rho_{p1}}} = \frac{\sqrt{\rho_{p1}}}{\sqrt{\rho_{p2}}} = \sqrt{\frac{\rho_{p1}}{\rho_{p2}}}. \tag{5}$$

This theory is adapted to the real world of finite rod length by assuming that results for endless streams of penetrator and target material also hold for a finite-length, rod-shaped penetrator attacking very thick armor material. The density law and the two assumptions made to this point suggest that a rod of steel of density 7.83 g/cm^3 should penetrate the same target material 1.49 times as deeply as a rod of tungsten alloy, density 17.3 g/cm^3, for the same striking velocity, mass and diameter. How close to this simple theory is reality?

2. EXISTING DATA

In the 1988–1991 time frame, the von Karman Facility's G-Range (VKFG) of the U.S. Air Force's Arnold Engineering Development Center, Arnold Air Force Base, TN, conducted a firing program in their two-stage light gas gun for the U.S. Army Ballistic Research Laboratory (BRL) Penetration Mechanics Branch (PMB), Terminal Ballistics Division (TBD), under the author's oversight (de Rosset, Sorensen, and Silsby 1991). An extensive penetration baseline was fired of tungsten sinter alloy rods, density 17.3 g/cm^3 (91W-6.3Ni-2.7Fe Teledyne Firth Sterling X27). Length-to-diameter ratios (*L/D*) ranged from 15 to 30, and masses were 125 and 250 g nominal. Targets were stacks of eight pieces of 3-in (76 mm) rolled homogeneous armor (RHA), retempered to the same hardness range as 6-in (150 mm) plate, and struck at normal incidence. By maintaining this hardness, the semi-infinite penetration performance baseline is consistent with a large class of data from the literature.

At the request of Konrad Frank of BRL, a shot was fired to look at the effect of density at high velocity. The 8.33-mm nominal minor diameter *L/D* 15 125-g rod, 125 mm long, was chosen as the baseline. To preserve mass and diameter, an 8.33-mm minor diameter × 276.07-mm-long 4340 steel rod was made. It was heat-treated to achieve an average Rockwell hardness of 45 (HRC 45), close to that of the tungsten rod. Striking velocity for this shot (VKFG 6461, fired 13 February 1989) was 2.97 km/s. Target hardness, averaged over the length of the penetration channel, had a hardness number on the Brinnel scale (HBN) of 268.5. A sufficiently low-yaw impact was obtained to guarantee reliable data (Bjerke et al. 1992). The depth of penetration was 247 mm.

Penetration per unit length of an unknown penetrator-target material combination can be approximated by multiplying the value of the penetration-vs.-velocity function for a known penetrator-target combination at the velocity of interest by the density law factor (Equation 5). One empirical relationship that fits the *P/L*-vs.-velocity data well, which I call a modified exponential form, is:

$$P/L = \frac{(B+CV)}{\left(1+De^{(EV)}\right)}, \tag{6}$$

where V is velocity in kilometers per second and B, C, D, and E are the fitting parameters. When applied to a set of 100 P/L-vs.-velocity data extracted from the literature and generated in-house (see Appendix A) for all tungstens of density 17.0–17.6 g/cm^3 into all semi-infinite steels of hardness approximately 269 HBN, one obtains:

$$P/L = \frac{\left(1.236 + 0.0875\ V\right)}{\left(1 + 117\, e^{(-3.5\ V)}\right)}. \tag{7}$$

This four-parameter fit is, of course, grossly overparameterized. This form was adopted to replace an earlier six-parameter hyperbolic fit that had the disadvantage of being negative at low velocities, making it perform poorly in regressions. The –3.5 and 117 values are arbitrarily fixed in Equation 7 to approximate the values that would be obtained at the absolute minimum standard deviation as determined by a free fit. Then A and B are treated as two free parameters.

The empirical modified exponential form matches reality much better than the physically-based Tate-Alexseevskii (T-A) fits, which use experimentally derived values for target and penetrator resistances to modify Bernoulli's equation for the impact of two coaxial streams of fluid of equal areas. The modified exponential fit is flexible enough that it closely follows many reasonably well-behaved sets of penetration data, and by constraining the parameter C to be positive, matches the observed, seemingly linear rise of P/L well beyond the hydrodynamic limit, which is crossed for tungsten-vs.-armor steel (P/L = 1.49) at about 3 km/s.

Based on this fit, penetration for the 125-mm-long tungsten baseline rod would be expected to be 186.7 mm at 2.97 km/s. Multiplying by the 1.49 factor for increased penetration due to increased length due to decreased density, the expected penetration depth for the steel-on-steel shot would be 277 mm (see Figure 1). Under this set of assumptions, the actual 247-mm penetration of the longer steel rod is 89% of the figure obtained by transforming actual tungsten-on-RHA data to form a predictor of steel-on-RHA performance by multiplying it by the density law factor. From another perspective, the steel rod did

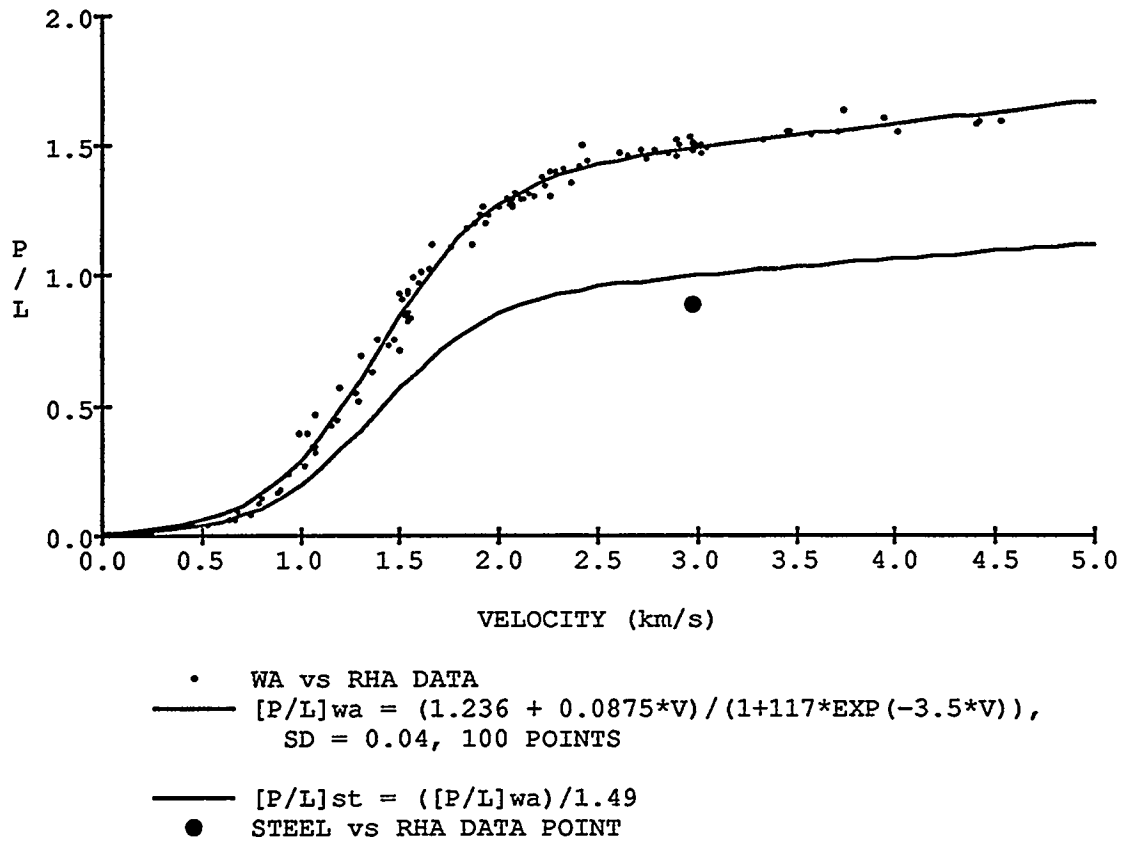

Figure 1. Tungsten long rod vs. steel hypervelocity database and modified exponential fit (see Appendix A, Table A-1). Lower line approximates expected performance of steel on steel resulting from dividing tungsten-on-steel curve values by 1.49. Point is actual performance of steel long rod.

32.3% better than its tungsten counterpart as opposed to 49%. There is some discrepancy between actual performance with this simplistic model in the lower end of the hypervelocity regime, and hence a discrepancy is almost certain in the lower-velocity regime as well.

The *P/L* for like-on-like strengthless materials should be unity. In this one case, the measured *P/L* was 0.89, showing some margin for improvement. But the increase in penetration of 32.3% on a mass-for-mass and diameter-for-diameter basis obtained through a decrease in rod density is quite an achievement, if the resultant longer rod can be successfully launched.

3. APPROACH

To explore the performance advantages of a holed-out rod, a number of experimental options were examined. The concept was thought to be particularly applicable to typical antitank long rod penetrators, necessitating a very long rod with small holes placed in a reasonably accurate pattern.

The concept was to be investigated in a modest in-house firing program. Ideally, small prototype rods, weighing under 100 g, would provide the potential for economically launching either tungsten or uranium alloys at velocities exceeding 2 km/s in PMB's quarter-scale ranges. This approach was first investigated by Lee Magness, a metallurgist in PMB with extensive experience in techniques for fabricating quite exotic small long rod penetrators. The best practical technique for making the small holes would be to cast, extrude, or swage a matrix of penetrator material surrounding a pattern of wires of a different material. The wires would then be preferentially etched away. However, this was deemed too costly and complex to consider further.

Gun drilling is a specialized process for machining a long, accurate hole that could be applied to manufacturing full-up rounds reasonably economically. To fabricate prototypes at a commercial facility, we would almost certainly be limited to a tungsten ballistic alloy as opposed to uranium. There is a lower limit on hole size that can be obtained that depends on the toughness and chip-forming qualities of the material to be drilled. Conversations with potential suppliers suggested that it would be possible to fabricate tungsten prototypes with a minimum hole diameter of about 4 mm, limiting testing to nearly full-diameter rods. Several suppliers could accurately place 500-mm-deep holes, but the lead time would be long. It was not thought necessary to fire full-length rods to evaluate performance.

PMB's Range 309A (R309A) was pursuing a program for Enderlein of BRL's Vulnerability/Lethality Division during his rotational assignment to BRL's Armor Mechanics Branch (AMB). He was firing 20-mm-diameter × 100-mm-long 555-g tungsten alloy short rods at ordnance velocities against a variety of candidate heavy armor backpack targets (Enderlein 1991). Specifically, the AMB rods were 92.87W-3.44Ni-1.51Fe-2.18Co (Teledyne Firth-Sterling X21C, produced by the large bar process, swaged 15% reduction in area, and strain-aged at 500° C for 1 hr). They had a density of 17.71 g/cm^3, a strength of 1.4 GPa, an elongation to rupture of 9%, and a hardness of HRC 47. Impact strength was 53 ft-lb (Poston 1990). All such rods serialized for firing in R309A were identified with a prefix of "2-."

This rod was well suited for a holed-out rod study. In the course of R309A sabot development work for Enderlein's program, two shots of the rod vs. RHA at normal incidence had been fired. Additional baseline shots needed for the holed-out rod program would benefit both parties. AMB kindly agreed to contribute the solid rods and other launch package components.

The number of holes, their diameter, and their placement fell out from other constraints. The larger the hole diameter, the easier the part would be to fabricate, with about 3 mm being the smallest hole diameter possible with commercially available tooling. The BRL shops were capable of drilling such holes in the tungsten ballistic alloy over 50 mm deep, so the pattern could be put into the 100-mm rod by drilling from both ends.

Concurrently with the experimental work, an extensive 3D computational effort using CTH on BRL's Crays was undertaken by Kimsey (1995). A pattern of eight holes was settled upon to provide an orthogonal pair of planes of symmetry through the rod's axis to decrease run-time by modeling only one-fourth of the rod.

A 1/8-in (slightly over 3 mm) hole diameter was selected to provide a large decrease in mass (to achieve 80% of the mass of the solid rod). An adequate web between adjacent holes and between hole and rod periphery was provided by situating the hole centerlines equally spaced on a circle 13 mm in diameter, the hole circle's center on the rod centerline. Several solid rod geometries were fired to provide benchmarks against which the performance of the lower apparent-density rods could be compared. Solid rods of the same length and mass as the drilled-out rod, 100 mm long × 17.82 mm diameter, would test the effect of length at full density. *L/D* 4 rods of the same diameter and mass as the holed-out rod would test the effect of mass at full density when their performance was compared with that of the *L/D* 5, 20-mm-diameter rods. See Figure 2 for rod dimensions.

4. EXPERIMENTAL RESULTS

The BRL Shops fabricated the various penetrators needed. These were fired from the 50-mm, smoothbore, high-pressure powder gun in PMB's Range 309A. A push-launch sabot was used, typical of the genre except with respect to a recently developed venting scheme whose details are unimportant here (Figure 3). A near-maximum propelling charge was used, so that striking velocity was about

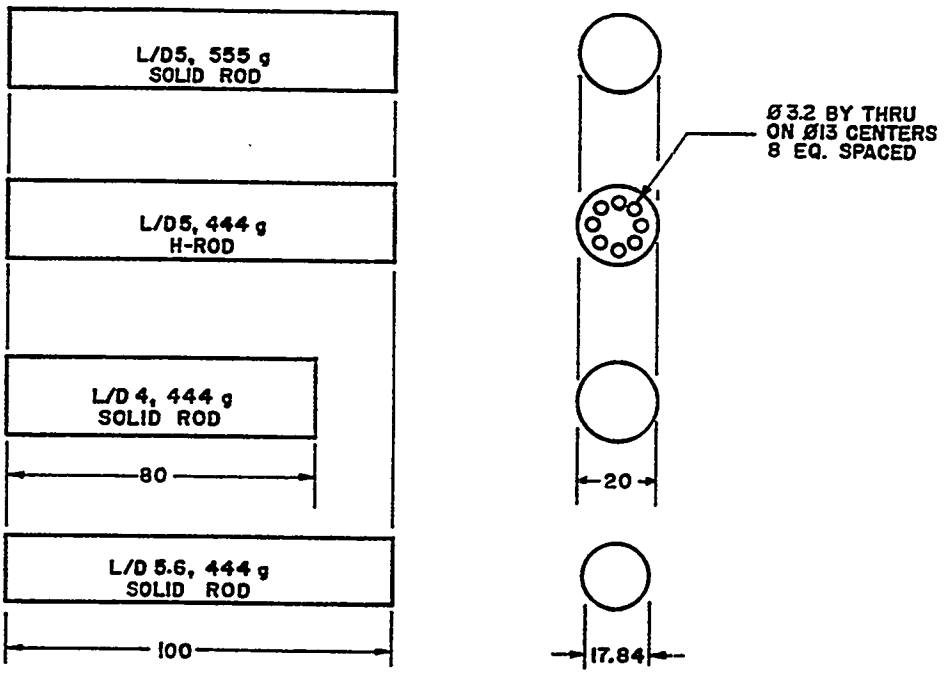

Figure 2. Rod geometries.

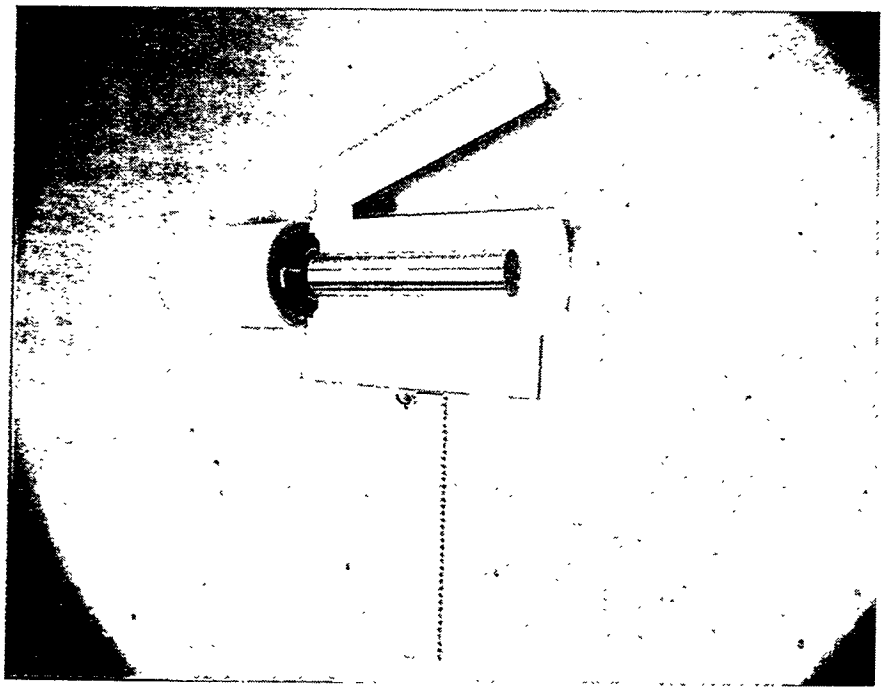

Figure 3. Push-launch package design for 50-mm, smoothbore, high-pressure powder gun, Range 309A.

1,600 m/s (Silsby 1995). The target was RHA at normal incidence. Targets would be sawed open to ensure accurate determination of the location of the channel bottom. It was hoped that velocity would be high enough that strength effects would not predominate, and the holed-out rod would penetrate just about as deeply as the *L/D* 5 solid rod.

Two aspects of the behavior of the holed-out rod were notable compared to the performance of the solid rods. The holed-out rod produced a clearly fluted hole in the target. And, the holed-out rod left no distinguishable piece of residual rod tail, unlike its solid counterparts.

The primary datum for making performance comparisons is the depth of penetration. The data from the H-rod program are tabulated in Appendix B, as well as additional R309A data for X21C rods vs. RHA used for further analysis (Table B-1). The bulk of these additional shots was undertaken by R309A under the author's supervision in the course of improving range capabilities. Several shots were conducted for AMB customers, who graciously consented to the use of their data here.

To be competitive on an equal-mass, equal-diameter basis, the holed-out rod had to penetrate at least as well as the *L/D* 4 444-g solid rod. It was hoped that it would penetrate nearly as deeply as the *L/D* 5 555-g solid rod (i.e., penetration was being driven by rod length, not momentum). In penetrations averaging about 100 mm, the data scatter (standard deviation around a straight-line fit) from the 100-mm-long, 444-g holed-out rod exceeded 13 mm, while that of the fits to the *L/D* 4 and 5 solid rod data barely exceeded the measurement precision at 2.5 mm each. Because of the holed-out rod data scatter, quantitative comparisons are problematic. The penetrations are plotted in Figure 4.

Qualitatively, the holed-out rod penetrated considerably poorer than the equal-length, 20-mm-diameter 555-g parent rod, and, on the average, a bit poorer than the 100-mm-long × 17.78-mm-diameter, 444-g equal-mass, equal-length solid version. In two shots, the holed-out rod did no better than the 80-mm-long × 20-mm-diameter, 444-g solid rod, considering the variability in the data sets. On the average, the penetration depth of the holed-out rod shots was somewhat above that of its equal-mass, 80-mm long × 20-mm companion.

A commonly accepted principle is that penetration per unit length increases smoothly with decreasing *L/D*—more so at lower *L/D*s, such as here, than for long rods (*L/D* > 10). When the penetrations were so normalized and plotted as a function of velocity, inconsistencies in the data became obvious. The 95%

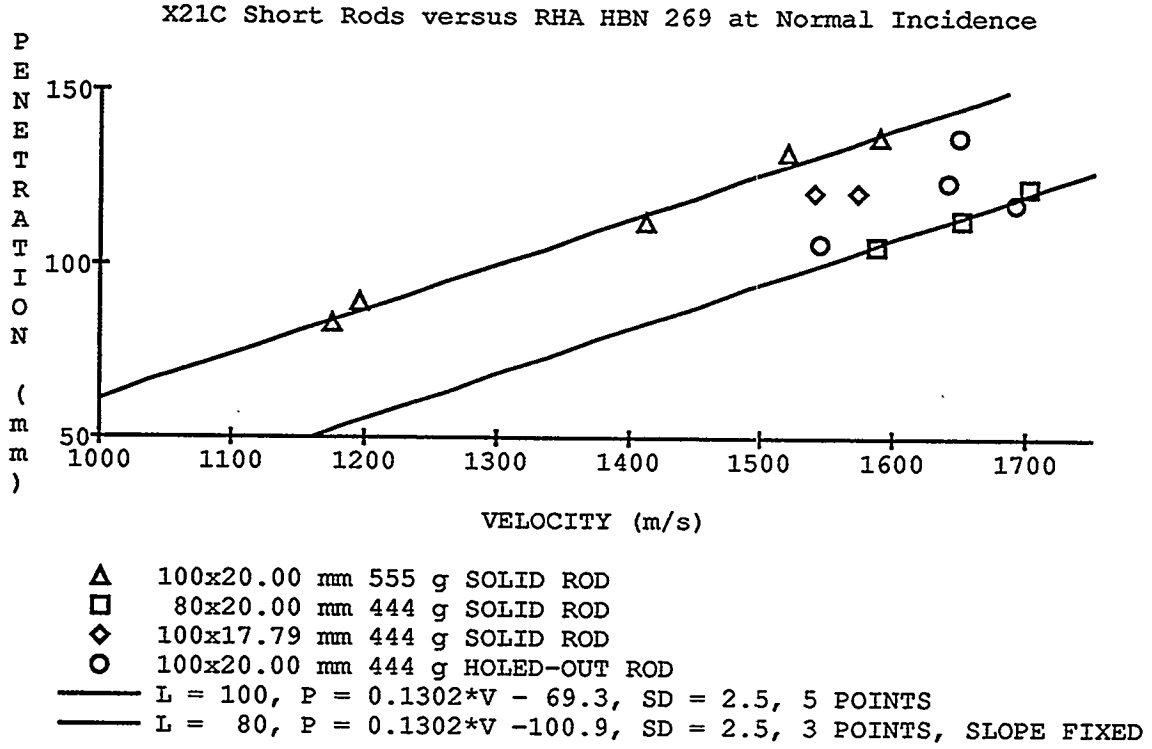

Figure 4. Penetration vs. velocity for various rod geometries.

confidence region around the data for the *L/D* 5 100-mm-long × 20-mm-diameter rod data included the *L/D* 4 data (80 mm × 20 mm diameter), even though both scatters were low. The *L/D* 4 data lay between the *L/D* 5 and *L/D* 5.6 (100 mm × 17.78 mm diameter) data (see Figure 5).

The excessive scatter in the holed-out rod data and lack of consistent rank-ordering of the penetrations by rod *L/D* suggested problems in the experimental technique. Further analysis of the data was indicated to surface and deal with the sources of variability in the data to establish a firm basis upon which to interpret results.

5. ANALYSIS

A number of causes of data variability suggested themselves. Additional X21C vs. RHA data were sought from the R309A database. Much of it was generated from time to time in the form of test shots following upgrade work on the gun or range (Appendix B, Table B-1, including measures generated in the analysis), with the exception of data from two baseline shots for Perciballi (1992) and one for Keele

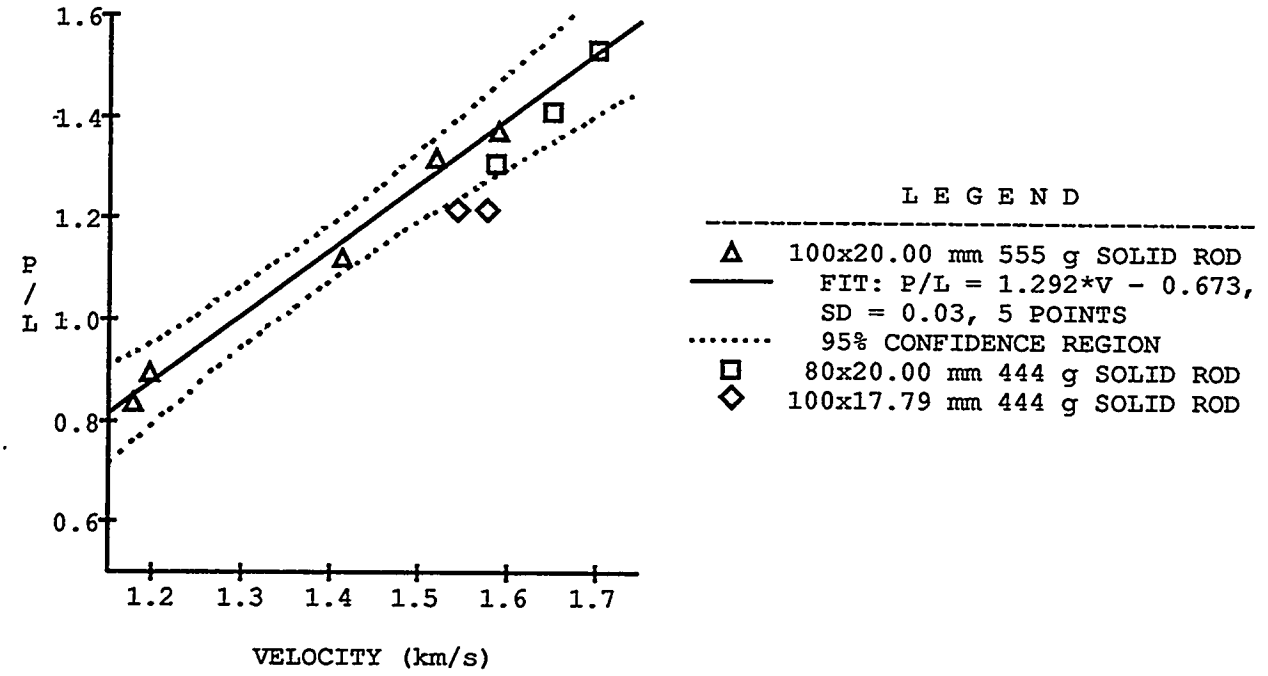

Figure 5. Penetration normalized by rod length vs. velocity for the same data set.

(1992), both of AMB.* The database was small and not homogeneous, so that the magnitude of some effects could not be determined or separated from others directly.

5.1. Yaw, Target Hardness Eliminated as a Source of Variability. The effect of yaw is well understood (Bjerke et al. 1992) and could be eliminated by excluding from analysis shots exceeding a computed threshold. Likewise, the effect of target hardness, well modeled by a multiple linear form around the velocities and hardnesses used in this program (Enderlein 1991), was eliminated by excluding from analysis shots from the database in which target hardness was not close to the nominal HBN 269 for 6-in (150 mm) RHA.

5.2 Other Influences Sought. The influence of other factors is less well understood. The data was inspected to surface any other obvious correlations. Assume that the measured *P/L* is the result of a series of factors, each proportional to some uncontrolled influence, multiplied by the *P/L* that would obtain if all factors were constant, the ideal behavior. (This assumes only a small interaction between factors.)

* Permission to use this data is gratefully acknowledged.

$$P/L_{meas} = f_1 \times f_2 \times f_3 \times \cdots f_n \times P/L_{ideal} \tag{8}$$

By averaging a lot of nearly homogeneous data in which the unknown influences are either small and well distributed or few and far between, the ideal behavior can be approximated. Thus, the fit to the large tungsten and steel long rod database, Equation 7, multiplied by some small factor to account for the rods in the database being softer and of lower density than the X21C data to be analyzed, is likely to be closer to the sought-after ideal X21C behavior in most cases than any function fit to the very small subsets of performance data for the X21C rods themselves. By dividing Equation 8 by Equation 7, the factors causing variability of the data are better exposed to view.

$$\frac{P/L_{meas}}{P/L_{fit}} = f_1 \times f_2 \times f_3 \times \cdots f_n \times \frac{P/L_{ideal}}{P/L_{fit}}$$

$$\frac{P/L_{meas}}{P/L_{fit}} \doteq (f_1 \times f_2 \times f_3 \times \cdots f_n) \times K \tag{9}$$

Comparing the average of these numbers between classes of possible influence, some conclusions can be drawn about the importance of each suspected component of variability. This can clearly be seen in the case of *L/D*. Numbers that stand out from their class suggest correlations with particular factors when consistently associated with variations in measures of possible causes of influence.

The pusher plate can create a significant dent in a target, possibly increasing the depth of penetration on certain shots. A technique for deflecting the pusher plate off the shot line was developed in R309A, eliminating this suspected source of data variability. For analyzing data acquired previously, a pusher plate damage measure was defined as the product of the mass of the pusher plate, an orientation factor that increased as the striking attitude went from flat to edge-on, and the estimated percentage of pusher plate that actually entered the penetration channel. No effect could be noticed.

This screening approach works only when one factor is predominant. It also cannot discriminate when there is little variation in suspected factors, in small data sets, or where one factor balances out another. Other suspected causes of variation in penetration would be whether or not the target was heavily backed

up in the axial direction, whether or not the target was comprised of multiple plates (laminated), and whether or not the penetration channel crosses one or more plate boundaries. There was insufficient data to settle any of these questions, and, in fact, much of the data in the literature may suffer from these influences.

5.3 Inadequate Lateral Confinement, *L/D* Effects Suspected. Work in progress by Lori Pridgeon (1995) of ARL quantified the effect of lateral target extent for *L/D* 20 65-g tungsten alloy rods attacking square RHA targets well centered. Her work shows an approximately 20% increase in depth of penetration at nominally 1,500 m/s as the targets went from 6 in (150 mm) square to 2 in (50 mm) square. This effect was independently confirmed in the work of Littlefield et al. (1995) with *L/D* 10 65-g rods attacking HRC 269 4340 steel cylinders at 1,600 m/s. They obtained a 37% increase in depth of penetration as the ratio of target-to-penetrator diameter dropped from 20 to 5. In the holed-out rod and the supporting R309A data, 17–20-mm-diameter rods were shot into 200- or even 150-mm-wide plates, so that the effective target-to-penetrator diameter varied, and could be as low as 7.5. On some of our tests, the shot-strike was significantly eccentric, thinning further the web of material around the periphery of the target at one spot. This reduced (and variable) lateral confinement became a major post-test concern.

Usually, the shot struck centered in a square target. As Pridgeon's data suggested, the width of the target was too small to be representative of a semi-infinite penetration. Analyzing Pridgeon's data suggested that a simple hyperbola of the form $P/Po = F/A + G$, described the increased penetration with decreased lateral extent. P/Po is the ratio of penetration into a target of decreased lateral extent divided by penetration expected for a very wide target, F and G are arbitrary constants, and A is the target presented area. A plot in Littlefield et al. (1995) for targets of a cylindrical geometry struck coaxially appears to behave similarly.

In the case of an eccentric shot line, plastic work in the target is not distributed symmetrically. See Figure 6. Localized zones of gross plastic flow at the thinnest webs could possibly reduce target penetration resistance further, but not enough data in this and related work could be surfaced to form a judgment as to just how to model the effect. Instead, the response was assumed to be hyperbolic as well, and the residuals examined to see if this assumption were justified.

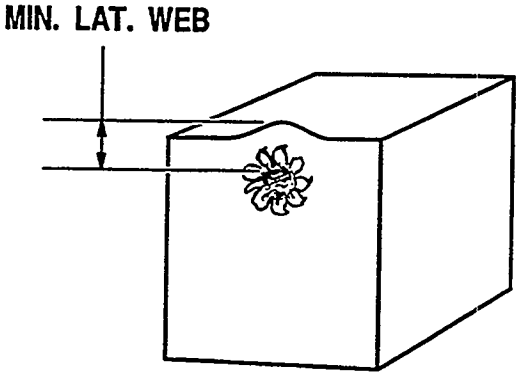

Figure 6. Target (least) lateral web defined.

For low *L/D* shots, the relief wave off the target face would be expected to contribute more to reduced penetration resistance than the effect of lateral confinement. Indeed, the unit penetration on the lowest *L/D* shots is generally higher than the global average of the R309A data set, showing this *L/D* effect. The effect of *L/D*, however, disappears into the noise in this data set at very low *L/D*s.

The effect of lateral confinement on the longer rod shots begins to be distinguishable from the noise when the ratio of minimum lateral web to projectile diameter drops below about two. The one holed-out rod shot with the suspected anomalously highest penetration also had the lowest ratio of lateral web to rod diameter, though still in the range of values of the comparable data.

5.4 Other Data Needed. The lateral confinement ratios (Column 24, Appendix B, Table B-1) for the holed-out rod data range from 3 to 4.25, while that of the *L/D* 5 data subset is about 2, that of the *L/D* 4 and *L/D* 5.6 data is about 4, and that of the lower *L/D* data around 2.5. It is impossible to analytically separate the effect of *L/D* from that of lateral confinement using this data. To do so, a clean set of data was needed.

A smooth and tractable mathematical relationship was sought to model the effect of *L/D* on *P/L*. Fortunately, an extensive collection of data could be assembled for tungsten alloy rods, density 17.6, attacking RHA-like semi-infinite steel targets, hardness nominally HBN 269. Data from Bjerke, Zukas, and Kimsey (1991) covered *L/D*s below 1 at 2 km/s. Though for a slightly less dense alloy (X27,

ρ 17.3 g/cm^3), it covers the low end of the range well, a necessity for determining a workable form. An extensive database from Hohler and Stilp, collected in a report by Anderson, Morris, and Littlefield (1992), and unpublished data of Farrand and his associates at ARL (1995) cover the region $1 \leq L/D < 32$ for a wide range of velocities. Other data for short rods had either been generated by the author during facility upgrade work or was made available by ARL researchers who had used Range 309A. As the $L/D \leq 0.5$ Bjerke data was at a fixed velocity not too far from the nominal 1.6 km/s of the holed-out rod work, the rest of the data was analyzed and used to generate *P/L*s at 2 km/s to match it.

5.5 *L/D* Effect Surprisingly Small for Long Rods. The data so assembled was plotted and examined for internal consistency. In the Hohler and Stilp data, the P/L numbers for three *L/D* 9 points as reported in Anderson, Morris, and Littlefield (1992) fell well below the values for *L/D* 10 and greater numbers. Since unit penetration is expected to monotonically increase with increasing *L/D*s, this data subset was disregarded (Anderson later provided corrections for this data). The *L/D* 10 data for four separate test entries was examined and found to be homogeneous and was pooled. The disposition of Hohler and Stilp's *L/D* 32 data points was such as to lead me to believe that several points were uncharacteristically low, resulting in an unrepresentative fit, so that data subset was not used either.

Farrand's data was for $10 \leq L/D \leq 30$, firmly anchoring the other end of the sought-after distribution. His data was generated with $\rho = 17.6$ g/cm^3 65-g rods of lower strength than the X21C rods of this work, so first a correction for rod strength was made. Farrand's exceptionally clean data, pooled with the R309A X21C data and the notes accompanying its statistical analysis appear in Appendix C, Table C-1. His individual data sets could be fit well by multiplying the specific modified exponential fit to the 100-point database (Equation 7) by a single scaling factor *S*. It was found that the effect of penetrator hardness on penetration was weak at best, and possibly nil. A parabolic fit for *P/L* on *L/D* on Farrand's long rod data was good (Appendix C, Table C-2 and Figure C-1).

A data set from Perciballi (1992) for a short hemispherically nosed rod of 95W-3Ni-2Fe was used for additional independent confirmation. The RHA penetration numbers were fit by a second degree polynomial and penetration at 2 km/s calculated. The overall rod length was reduced by one-sixth the diameter to adjust the length to that of a flat-nosed rod and a *P/L* formed. This corrected WA vs. RHA penetration number was reduced by a factor of the square root of the ratios of the densities to correct it to a nominal density of 17.6 g/cm^3.

The *P/Ls* for these different data, corrected to 2 km/s, were then plotted. They can be seen to increase slowly with decreases in *L/D*, until as *L/D* approaches 1, the curvature needed to fit the data increases rapidly. From a baseline *P/L* of about 1.2 at *L/D* 30, it is up to about 1.5 at *L/D* 5, then to 2 at *L/D* 1. *P/L* continues up with increasing *L/D* in the region of Bjerke's (lower density, lower strength!) data, peaking at about 4 (with lots of scatter) at *L/D* 1/8, then dropping towards zero as the discs get thinner. It is hard to plot the behavior on a single graph and still see the effects discussed. Figure 7 shows the data plotted linearly, Bjerke's *L/D* 1/4 and 1/8 data points being averages of the *P/L* values of 4 and 3, respectively.

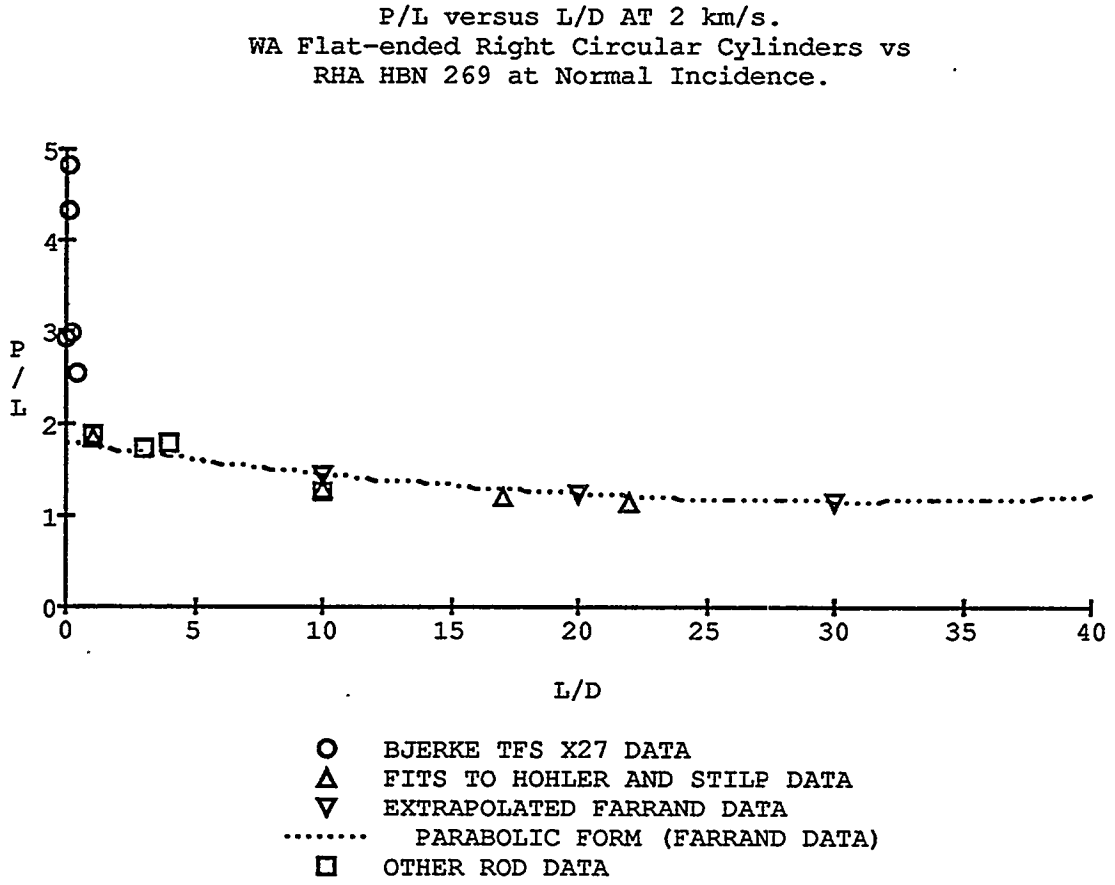

Figure 7. Raw *P/L* vs. *L/D* relationship. Points usually represent calculated values and not individual data.

Even so radical a function as that used by Planck to model black body radiation failed to rise quickly enough from zero to be able to force a fit through both the rising and falling limbs of the data. With the two lowest *L/D* points suppressed, that form was found to give the best fit of those tried. Figure 8 shows that fit plotted to a logarithmic scale. It is interesting to note that the parabolic form, the left limb of which matches Farrand's data so well, lies within the 95% confidence limits of the "black body" form

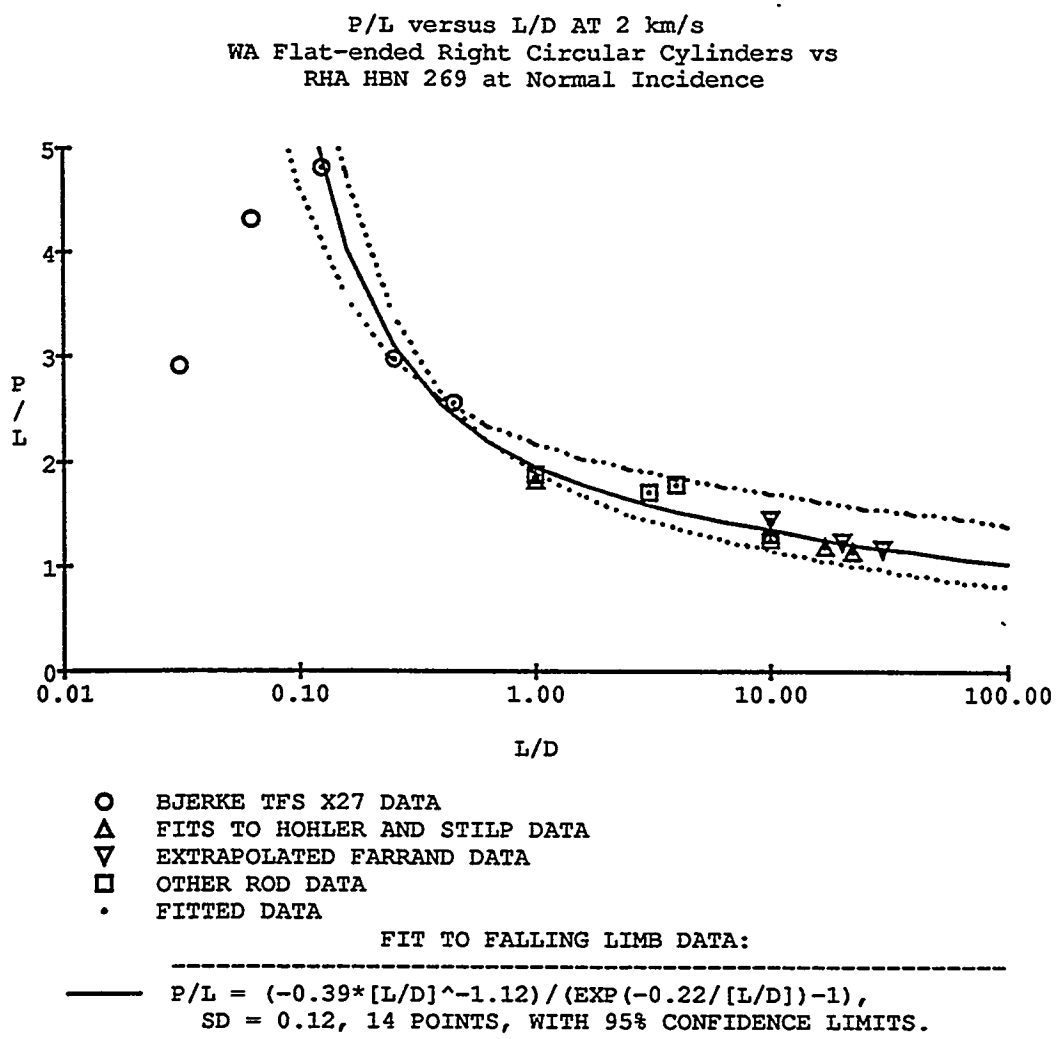

Figure 8. *P/L* vs. *L/D* fit for *L/D* > 0.01, plotted on log-linear scale.

fit to the data set with the two lowest *L/D* points suppressed until the decreasing *L/D* takes on a value of almost exactly unity. Over the interval for which they report data, this response is seen in another set of Hohler and Stilp's data (taken from the same reference) for shots into a significantly harder target steel.

In their work, Bjerke, Zukas, and Kimsey (1991) explain the peak in *P/L* vs. *L/D* as being due to a change in penetration from rod-like behavior to plate-like behavior as the diameter-to-length ratio gets large enough that the relief waves reach the penetration interface from the axial free surface sufficiently before relief waves from the radial periphery do. In the rod-like regime, the rod erodes by radial outflow of rod material, for *L/D*s over about 1. Below *L/D*s about 1/16, the plate rebounds off a normal incidence target by momentum trapping. A mixed mode regime exists between the two, in which a progressively larger central region of the penetrator is uneroded as the *L/D* decreases.

Fitting the *P/L* data for various *L/D*s as a function of velocity support the hypothesis of a fundamental change in the slope of the *P/L*-vs.-velocity relationship at a *L/D* value near unity. The use of a simple scaling factor serves well to adapt the modified exponential form to a wide variety of long rod and even short rod *P/L*-vs.-velocity data, but it does an unacceptable job for the *L/D* 1 data, as a free fit seems to want less curvature on the rising limb than for longer rod data. Applied to the Hohler and Stilp *L/D* 1 data, the exponent was almost 1.

5.6. Lateral Constraint Effect Consistent With Recent Results of Others. With the *L/D* effect being so weak, it is even more critical to account properly for the effect of lateral confinement. The fit suggested by Pridgeon's work indeed provided the lowest standard deviations to the R309A unit penetration data augmented by Farrand's data set. The form

$$P/L = f(L/D) \times f(V) \times (A + B/[Web/D]^n) \tag{10}$$

is overparameterized, which is to say that there is a strong interdependence among the parameters when fit. By setting some of them to values within their 95% confidence region and running a fit on the others, the standard deviation only varies around the lowest value by a few percent. The final form chosen was,

$$P/L = (1 + 0.000906 \times (30-[L/D])^2) \times f(V) \times (0.807 + 1/([Web/D]^2)), \tag{11}$$

where *Web/D* is the target lateral web, and the form constrained to $L/D \leq 30$. In most cases, *Web/D* is just half the target width, divided by rod diameter. *f(V)* is (the by now familiar) Equation 7. The standard error of the estimate of this fit is 0.093, with 69 data points. The residuals and notes regarding the fit are presented in the dataset in Appendix C-1. In this form, the two 1's and the powers of 2 are set arbitrarily, near values they want to take on in a free fit. Rather than increasing, the standard error of the estimate actually decreases by about 1% under these constraints.

The residuals to this fit are plotted against each independent factor (scatter plots) in Figure 9. One measure of a good fit is that the residuals are well disposed about the zero line over the entire interval. This holds for the lateral web case. There may be a very slight rising trend in the residuals plotted vs. *L/D* as *L/D* values increase beyond 20. A dipping and rising could possibly be discerned in the residuals plotted vs. velocity. Certainly, essentially all of the residuals are positive below about 1.4 km/s, with the rest of the data more or less well disposed except for a few outliers. Thus, the fit should not be relied on below 1.4 km/s. Since the primary area of interest in this work is 1.6 km/s, no further effort to massage the data was undertaken.

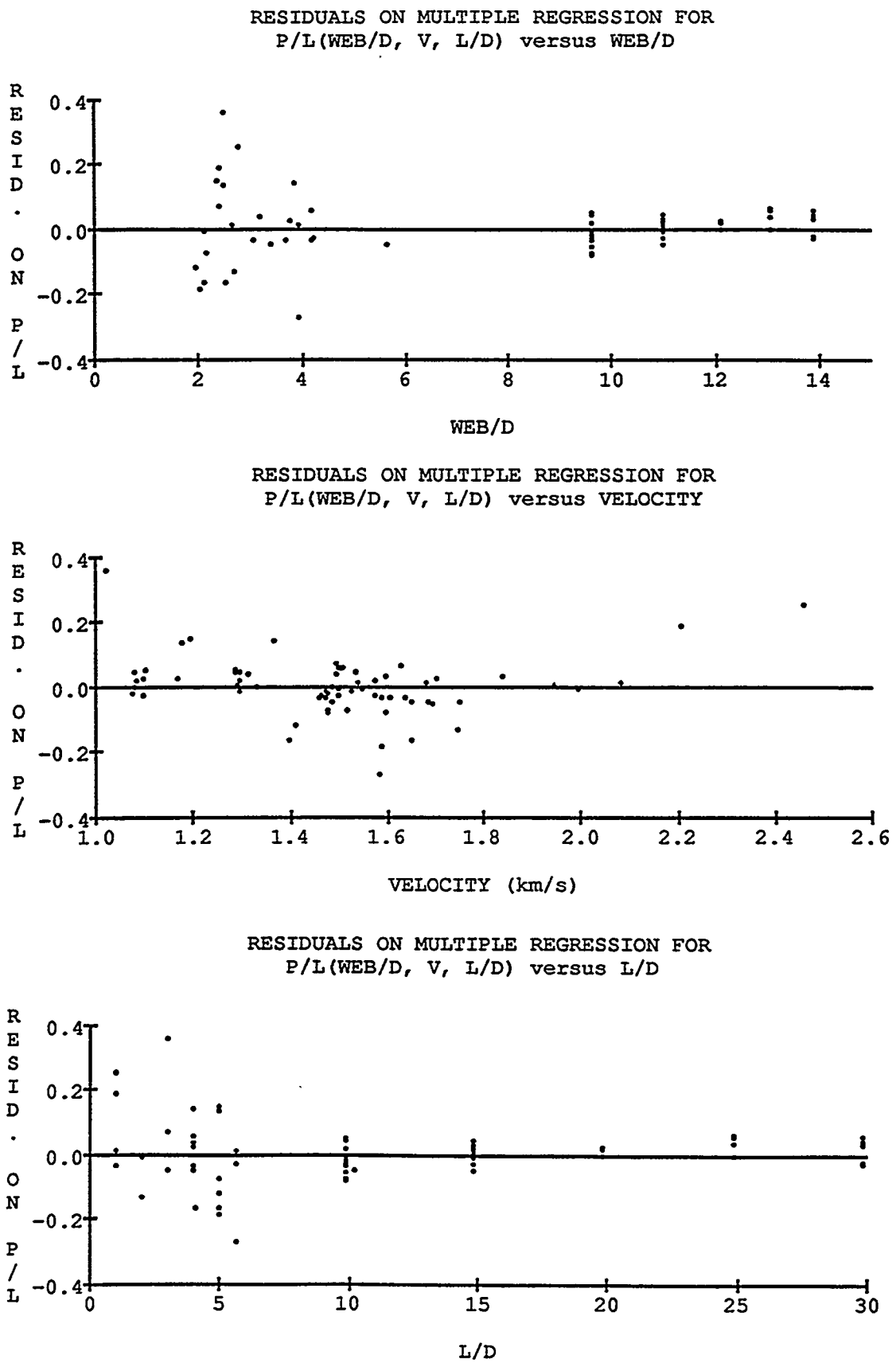

Figure 9. Scatter plots of residuals to multiple regression.

The lateral constraint term in Equation 11 was compared with the data of Pridgeon (1995) and of Littlefield et al. (1995) in the form of a graph, Figure 10. Given the limited data in both their sets, and the limited range, there is reasonable agreement. The confidence region on each parameter was rather tight in all fits, so that, for example, there is no question that each fit wants the power term given. However, altering or adding only a few points in each data set could cause that circumstance to alter. Remember that the "lateral web" term is just half the target diameter where the datum could not be measured. Thus, Web_t/D_p is just essentially $1/2 \times D_t/D_p$, t and p denoting target and penetrator, respectively. The three sets of data reflect three different target deformation situations. In the case of a circular target struck well-centered (Littlefield et al. 1995), the plastic deformation is uniform in any circumferential path. In a square target struck well centered (Pridgeon 1995), the plastic work is confined to four zones around the thinnest radial webs. In the case of a square target struck closer to one edge than any other (this work), the plastic deformation would occur predominantly in only one zone, where the web was thinnest. There is too little good data in my work to support any conclusions regarding this effect, but it is interesting and important and needs further study.

It is comforting to note that the effect of lateral confinement determined in this work is small until the lateral web drops below about 4, as the cursory examination of the data suggested, below which target penetration rises steeply. Note that the correction term for lateral confinement in this fit is independent of *L/D*, which it probably should not be. However, we will use this fit primarily at *L/D*s of 4 and above, where discrepancies should be reasonably small. Note also that the fitted parameters are independent of velocity, which may or may not be true.

5.7 Predicted Behavior for Large Targets. Equation 11 can now be used to generate expected performance predictions for X21C rods attacking very large (width and height) RHA at normal incidence. Being (assumed) independent, the individual factors derived from the multiple regression may be used to correct individual data for particular effects. Figure 11 shows the correction for lateral confinement applied to the baseline data set, which was plotted earlier in Figure 4. The raw data are plotted as open symbols, and the corrected data are plotted as filled symbols.

Observe that the overall scatter in the data is reduced, a sign that the influence sought is actually there. The corrected *L/D* 4 and 5 data converge towards the origin, more in line with reality than the parallel slopes in the raw data. Further, the correction to the *L/D* 5.6 data brings its slope parallel and essentially coincident to the *L/D* 5 fit. This is an improvement over the raw data, in which the raw *L/D* 5.6 penetrations lay between the raw *L/D* 5 and 4 data, contrary to expectations.

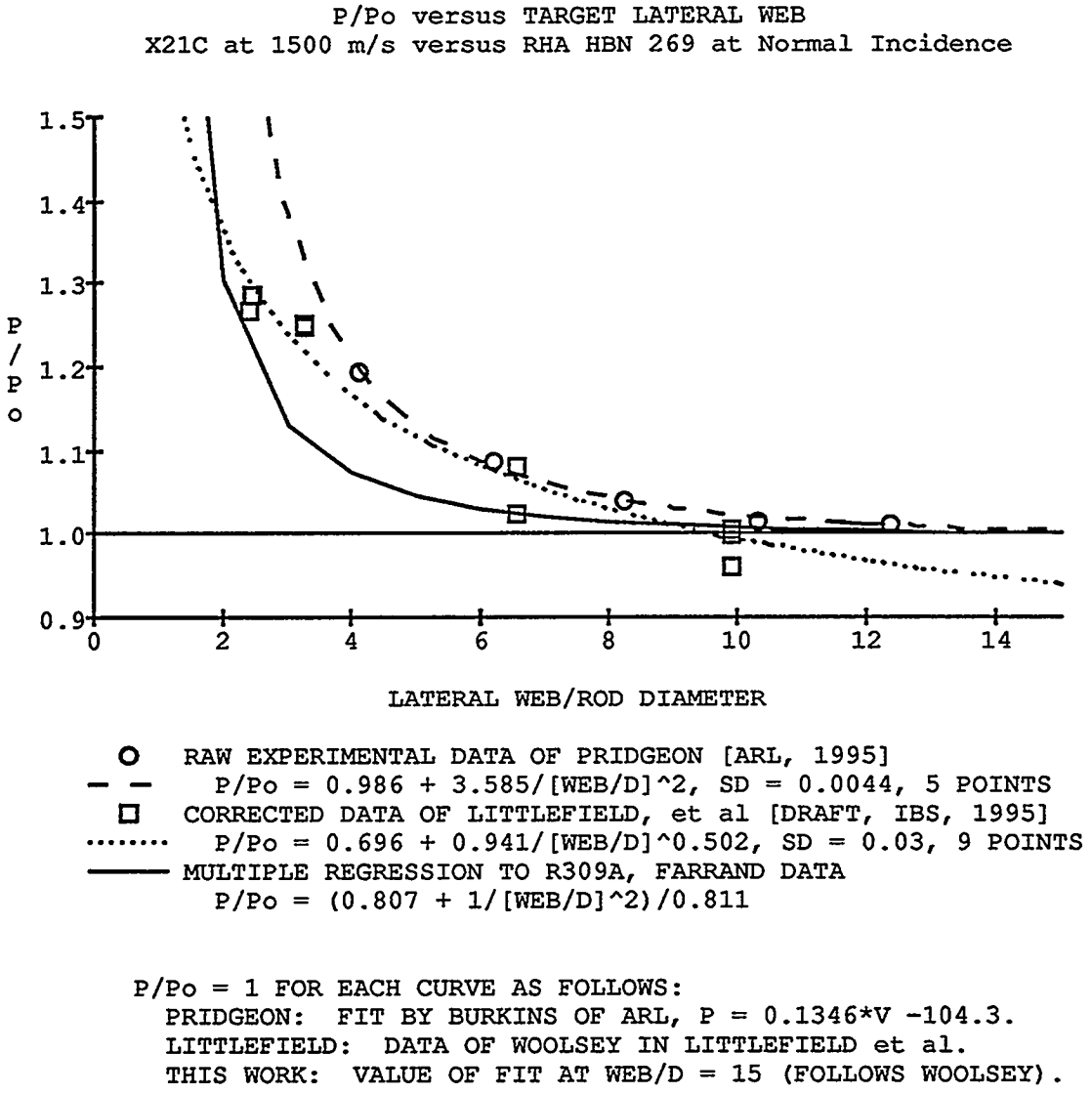

Figure 10. Increase in penetration with decrease in lateral confinement at 1,500 m/s.

Note, however, that the correction to the *L/D* 5 data seems to be excessive at lower velocities, as suggested by the velocity scatter plot (see Figure 9). The reduction in penetration should diminish as velocity decreases. This is undoubtedly the result of assuming that the influence of velocity can be corrected by simple vertical scaling of the a particular sigmoid curve. This would be less the case if the correction scheme allowed the baseline curve to be shifted horizontally at the low end of the velocity regime rather than vertically, for example, consistent with the two-parameter analytic formulation (after

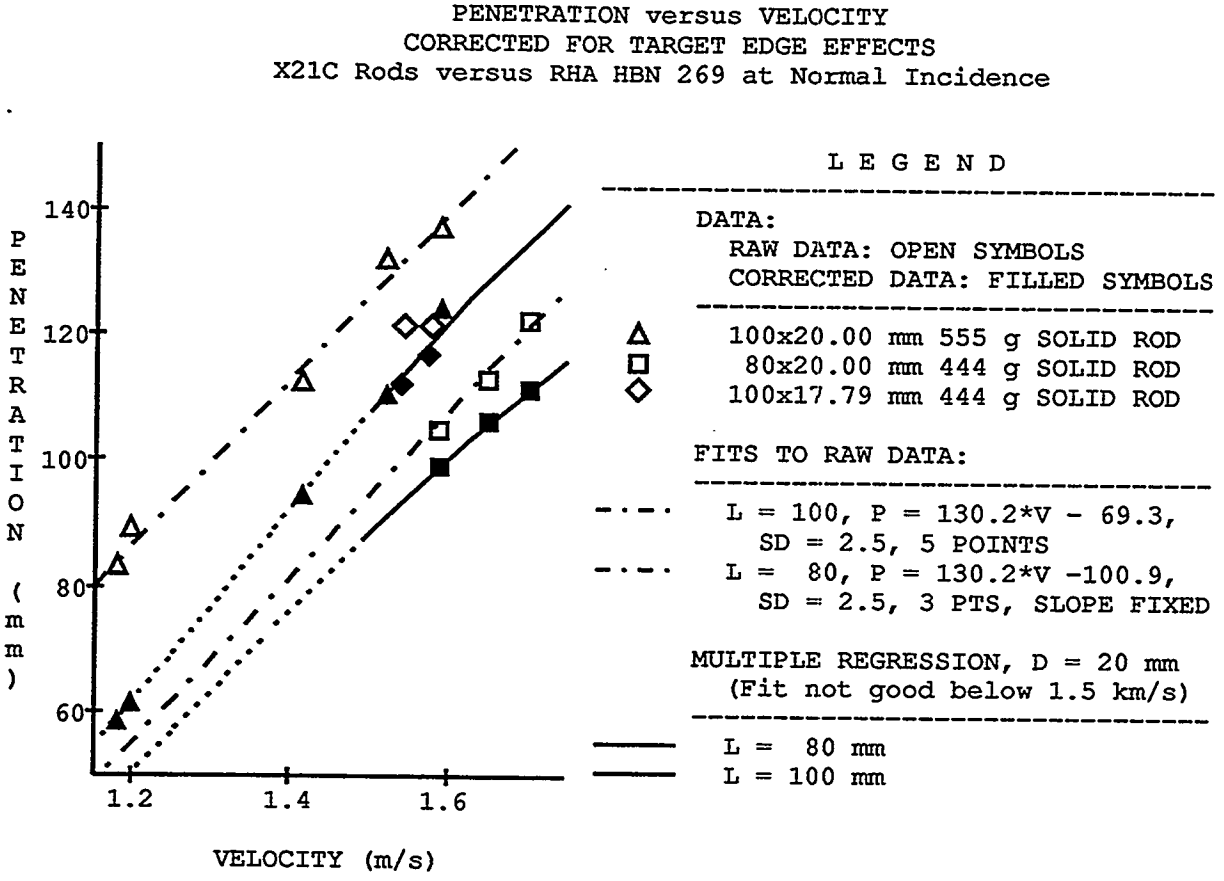

Figure 11. Penetration data corrected for target lateral confinement.

Lance and Odermatt) presented by Rapacki et al. (1995) in their paper at the 15th International Symposium on Ballistics.

Nevertheless, the correction scheme appears good in the region of interest, between about 1,500 and 1,800 m/s. This is reflected on the graph by using a solid line for the final form only in the areas of interest. The corrected data, including that of the holed-out rod, are replotted at finer scale in Figure 12. A line is fit to the holed-out rod data, and the standard deviation of the fit decreases from 13 mm to 8 mm, again suggesting that reduced lateral confinement had a positive correlation to increased penetration. This decreased scatter contributes to increased confidence in the conclusions drawn, but in our case, as discussed later, the scatter is still poor. The values that will be used for comparison among the various cases are those obtained at 1.6 km/s. These are tabulated in the discussion.

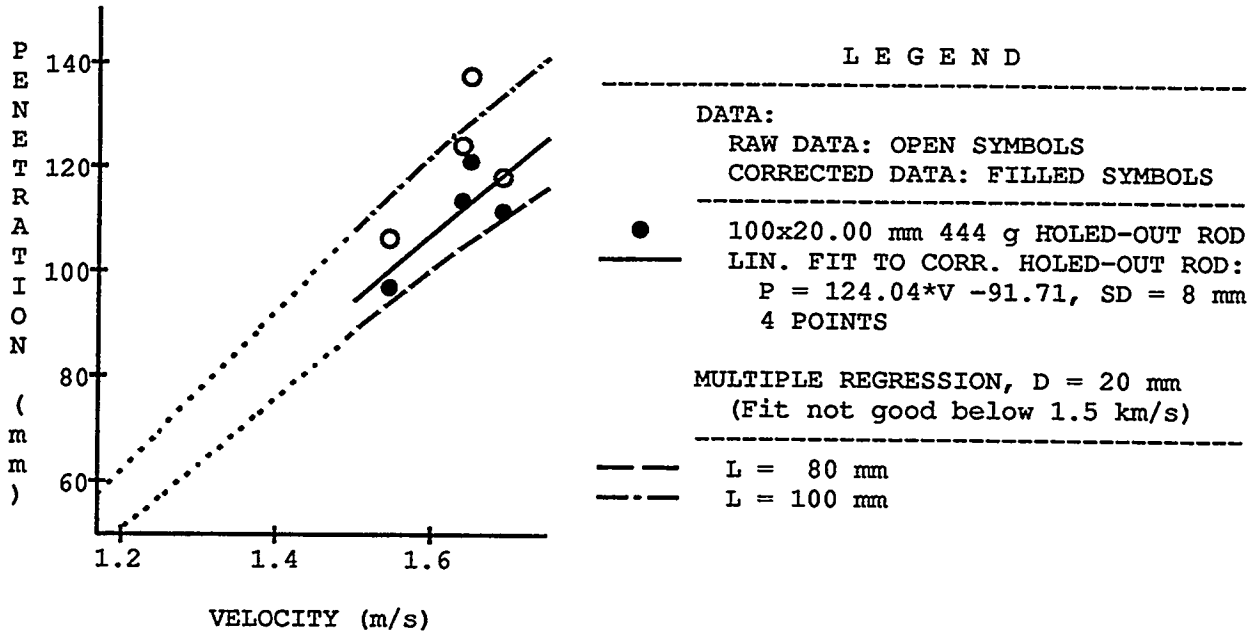

Figure 12. Penetration of holed-out rod compared with baseline. (Corrected values.)

6. INTERPRETATION

With the corrections, the penetration of the 100-mm-long × 17.79-mm-diameter, 444-g rod is the same as that of the 100-mm × 20-mm-diameter, 555-g rod, suggesting that length is the predominant factor, not diameter, in this velocity regime.

The penetration of the *L/D* 5 100-mm-long × 20-mm-diameter, 555-g rod at 1.6 km/s is 23% greater than that of its *L/D* 4 80-mm-long × 20-mm-diameter cousin, showing the small effect (3%) of *L/D* after the 20% effect of length is removed. The penetration of the holed-out rod is only a bit higher than that of the equal-mass *L/D* 4 solid rod, implying poor performance for the holed-out rod. Given the scatter in the holed-out rod data, there is some likelihood that additional shots would cause significant changes in the location and slope of the fitted line, and it cannot be stated confidently that the 20% longer holed-out rod actually performs any better than its equal-mass *L/D* 4 solid cousin.

John Zook (now retired) and Konrad Frank of ARL collaborated to generate predictions on the penetrations to be expected in these cases using the T-A model. In this model, the holed-out rod is modeled as a solid rod of the same outside envelope and lower mass (density). The overall relationship

among the results of the T-A model was in good agreement with the overall relationship observed, though there is sufficient disparity in the absolute numbers that the model is clearly too simple. Table 1 shows the results (Zook and Frank 1991).

Table 1. Corrected Fit to Data Compared With Tate-Alekseevskii Predictions of Zook and Frank. Velocity is 1.6 km/s. Zook and Frank used a penetrator density of 17.3 g/cm^3 vis-a-vis measured values of 17.65 g/cm^3 in this work.

Case	Corrected Penetration (mm)	T-A Pred. Penetration (mm)
100-mm-long × 20-mm-diameter solid rod, 555 g, *L/D* 5	122.1	105
100-mm-long × 17.84-mm-diameter solid rod, 444 g, *L/D* 5.6	118.6	102
80-mm-long × 20-mm-diameter solid rod, 444 g, *L/D* 4	100.5	88
100-mm-long × 20-mm-diameter holed-out rod, 444 g	106.6	86

Both the model and experiment showed only a slight decrease in penetration for the 100-mm-long solid rod as diameter dropped from 20 mm to 17.84 mm (16.70 mm in the T-A model), while mass dropped 20% and *L/D* increased from 5 to 5.6. Both the model and experiment showed essentially identical performance of the 80-mm-long *L/D* 4 solid rod and its equal-mass, 100-mm-long counterpart of lower apparent density.

Kimsey's (1995) computational effort was undertaken to understand the physical mechanisms involved and to improve the models. Runs were done at 1.6 km/s to match the experiments, and at 2.5 km/s to see if the performance would improve at higher velocities.

As with the corrected data, at 1.6 km/s, CTH predicted that the *L/D* 4 solid rod and holed-out 444-g rods would perform essentially the same, while the *L/D* 5, 555-g solid rod would penetrate approximately 20% better. CTH only slightly underpredicted penetration for all 1.6-km/s cases. At 2.5 km/s, where no experimental data is available, CTH shows about a 10% deeper penetration for the drilled-out rod over the equal-mass *L/D* 4 solid rod. The results are underpredicted compared to the curves for corrected experimental data. See Figure 13.

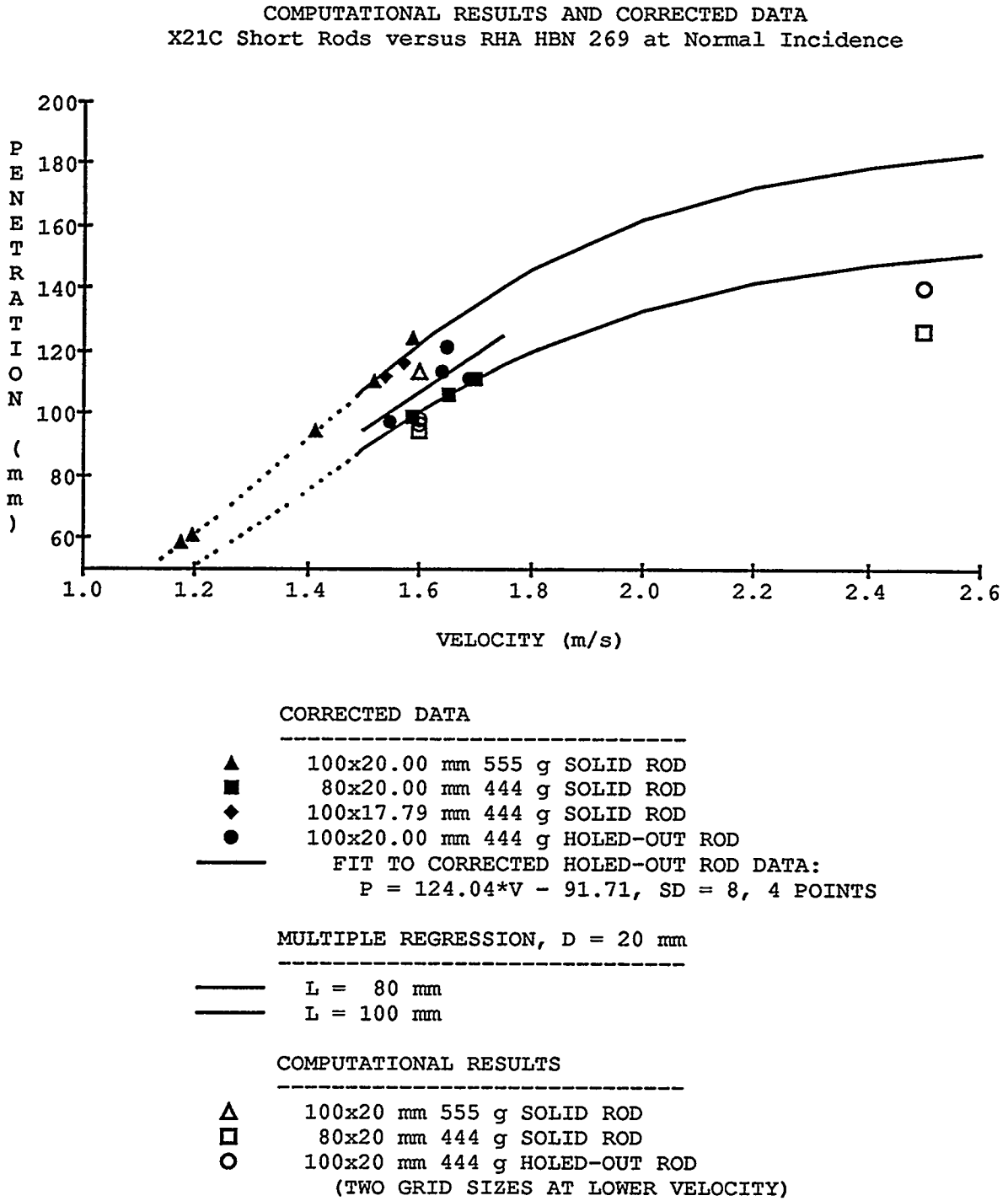

Figure 13. Numerical predictions compared with corrected data.

7. TUBULAR PENETRATOR INSIGHTS

Why is the holed-out rod underperforming compared with a simple reduced-density model? The penetration mechanics of the reduced-mass penetrator concept are related to the impact dynamics of tubular penetrators, which have been studied since at least 1960. Frank and McLaughlin (1978) have reviewed and summarized most of the early tubular penetrator research conducted at ordnance velocities. Payne (1968) and Sanders (1970) report ballistic test data for hypervelocity impact of thick-walled tubes (ratios of inside to outside diameter, w, from 0.5 to 0.65) of steel, aluminum, and titanium impacting aluminum and steel targets. Hough (1982) used the HULL code to compare penetration-time histories of RHA tubes, $w = 0.8$ and 0.6, as well as a rod attacking RHA at 1.2, 1.6, and 2.0 km/s out to 30 μs. Recently, Franzen of California Institute of Technology (1987), and Franzen and Schneidewind (1991) reported results of analytical modeling, hydrocode calculations, and ballistic tests of hypervelocity tubular penetrators. Franzen observed that the penetration depth per consumed penetrator length is a steady-state process which is dependent on the ratio of inner to outer tube diameter, the ratio of tube material to target material density, and impact velocity.

In the tubular penetrator work cited, the presence of a zone of reduced pressure at the core of the penetration reduces the relative erosion rate of the target. The extensive computational work by Kimsey reveals that the holed-out rod is underperforming precisely because of the hole pattern needed to decrease the penetrator mass. The reduction in pressure occurs in an annular zone away from the centerline, but the effect is the same: reduced relative erosion rate of target to penetrator. The reduction in pressure at the penetrator-target interface occurs at a reduced radius compared to that of a solid rod. Beyond this radius, the material from the periphery of the holed-out rod impacts too far away for the pressure under that material to influence the central penetration in progress. The peripheral material is, in effect, wasted. In the tubular penetrator, if the holes could be made small enough, penetration would not suffer much. In the holed-out rod, if the area of the holes is big enough to achieve a meaningful reduction in apparent density, it is accompanied by a significant reduction in penetration.

The central core of the holed-out rod acts as a lower mass, higher L/D rod, which has a slightly lower penetration per unit length than rods of a lower aspect ratio. The material from the outer regions, rather than contributing to penetration, appears to just ride on the surface of the eroded rod material, flowing radially out from the core and not contributing to penetration.

8. CONCLUSIONS AND RECOMMENDATIONS

In this work the penetration of a reduced-mass (reduced apparent density) low *L/D* penetrator, achieved by drilling a symmetric pattern of eight holes parallel to the rod's axis, was compared with that of several comparable solid tungsten alloy rods. The central trend of the data for the holed-out rod fell only slightly above the depth expected for rods of equal mass and equal outside diameter. Given the increase in sabot mass needed to carry this additional length, there is a negative incentive to lengthen the rod by holing it out. This performance is consistent with independently generated predictions by Zook and Frank (1991) and with CTH runs by Kimsey (1995).

The approximately 10% increase in penetration over the equal-mass, shorter cousin at 2.5 km/s is interesting, but even then, such a gain could be achieved by lengthening the baseline rod proportionately and it would still be 10% shorter than its holed-out cousin. It is doubtful that the additional parasitic (sabot) mass needed to launch the longer holed-out version could be reduced enough that the throw-weight of a holed-out launch package could be brought under that of a monolithic rod of equal terminal ballistic performance.

There is one speculative advantage to the holed-out penetrator concept that remains untested. Reactive armor acts to deform the rod laterally, imposing a finite lower limit on rod diameter. While having the same cross-sectional area and hence the same strength in lateral shear, the higher bending stiffness of the holed-out rod concept should permit it to survive under higher lateral bending forces than the longer and thinner option.

Given the limited number of holed-out rod data and their large scatter, even after corrections were made for target edge effects, conclusions cannot be drawn with any real confidence. The 95% confidence region around a straight-line fit to the holed-out rod data engulfs essentially the entire quadrant, in contrast to the 95% confidence limits drawn around straight-line fits to the 80-mm- and 100-mm-long solid rod data. See Figure 14. Confidence limits are drawn around the straight-line fit to the holed-out rod data at the one-in-two, one-in-four, and one-in-eight levels. These represent regions outside of which a straight-line fit to a data set represented by the four shots could be expected to fall at these probability levels. Thus, while it is reasonably certain that the holed-out rod and 80-mm solid rod data are from populations with indistinguishable central trends, there is still approximately one chance in eight that more shots would shift the mean to a point where it is indistinguishable from the 100-mm-long solid rod data.

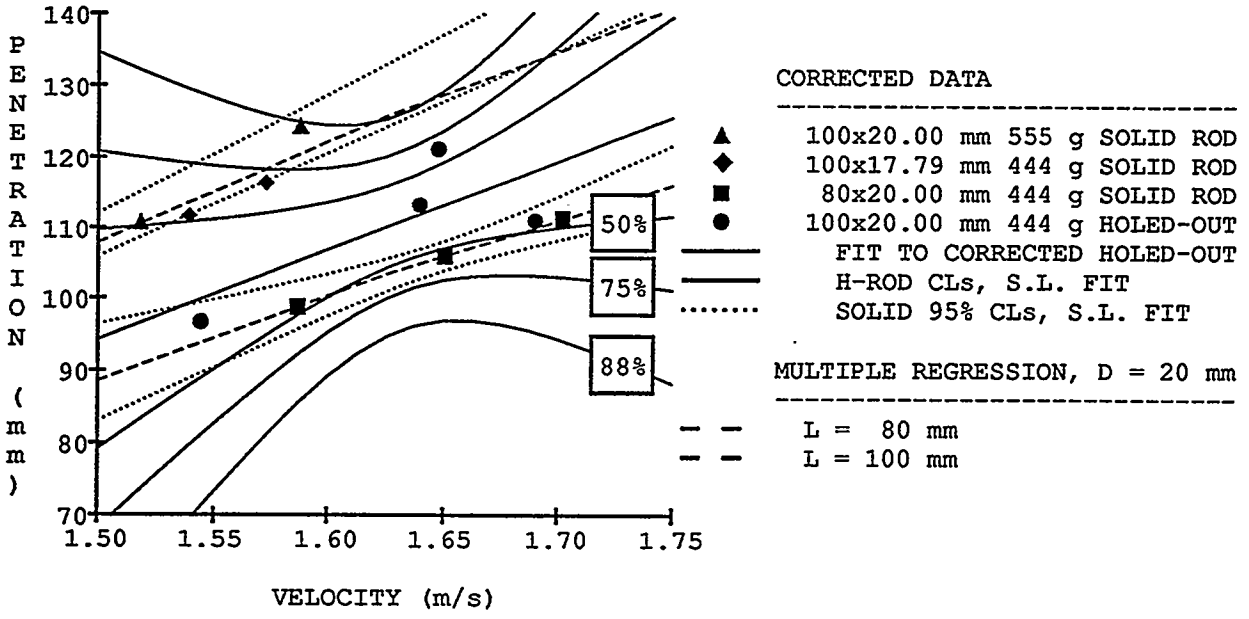

Figure 14. Confidence intervals around straight-line fit to holed-out rod data.

Should it be desired to consider pursuit of this matter at full-scale, additional reduced-scale shots would be very wise. This would allow an attempt to be made to eliminate the source of the data scatter upon which such a scale-up decision need be made. They should be fired at two velocities: as high as possible and at a reduced velocity to maximize the velocity spread and hence reduce the fan-out of the confidence regions around the currently limited data set. Additionally, depending on observed data scatter, *L/D* 5 drilled-out rods should be fabricated and shot at 2.5 km/s to verify the CTH predictions. Then sufficient long drilled-out rods should be fired at as high a velocity as practical to measure both the sought-after performance increase and its variability.

Full-scale shots of 20-mm diameter X21C tungsten alloy holed-out rods could profitably be conducted at *L/D*s of as little as 10, for which the *P/L* values have risen only about one-third above that of the very-long rod value (see Table 2). Long holed-out rods could possibly be fabricated by inertial welding two *L/D* 5 holed-out rods, possibly cutting fabrication costs significantly.

For an approximately *L/D* 10 900-g rod, two types of launch platforms are available. Full-scale laboratory guns at BRL can be used, using current laboratory sabot technology to achieve a maximum of

Table 2. Projected Solid Rod RHA Unit Penetration. (From multiple regression, ratio of target lateral web to rod diameter of 15.)

L/D	*P/L* at 1.6 km/s	*P/L* at 2.5 km/s
5	1.221	1.815
10	1.062	1.579
30	0.779	1.159

about 2.2 km/s. For higher velocities, a large-bore two-stage light-gas gun would be necessary. For example, the one at the Arnold Engineering Development Center's von Karman G-Range could deliver striking velocities in excess of 3.0 km/s. Experimental firings would require the design of a first cut sabot for both the solid and the holed-out rod, thus providing a firmer basis for comparisons of systems performances.

The correspondence between experiment, a simple physical model, and the sophisticated finite difference code CTH suggests that there is little likelihood of unexpected results if additional experimentation is undertaken. However, this effort has resulted in advances in understanding the penetration mechanics of holed-out rods.

INTENTIONALLY LEFT BLANK.

9. REFERENCES

Anderson, C. E., B. L. Morris, and D. L. Littlefield. "A Penetration Mechanics Database." SwRI 3593/001, Southwest Research Institute, San Antonio, TX, January 1992.

Bjerke, T. W. "The Effect of Material Strength on Segment Penetration Behavior." ARL-MR-51, U.S. Army Research Laboratory, Aberdeen Proving Ground, MD, April 1993.

Bjerke, T. W., J. A. Zukas, and K. D. Kimsey. "Penetration Performance of Tungsten Alloy Penetrators With L/D Ratios of 1 to 1/32." BRL-TR-3246, U.S. Army Ballistic Research Laboratory, Aberdeen Proving Ground, MD, June 1991.

Bjerke, T. W., G. F. Silsby, D. R. Scheffler, and R. M. Mudd. "Yawed Long-Rod Armor Penetration." International Journal of Impact Engineering, vol. 12, no. 2, pp. 281–292, 1992.

De Rosset, W., B. Sorensen, and G. Silsby. "Effects of Increased Penetrator Velocity, Part II." BRL-MR-3890, U.S. Army Ballistic Research Laboratory, Aberdeen Proving Ground, MD, January 1991.

Enderlein, M. W. "Armor Backpack Effectiveness Against Rod Penetrators at Ordnance Velocities." BRL-MR-3939, U.S. Army Ballistic Research Laboratory, Aberdeen Proving Ground, MD, October 1991.

Farrand, T., W. Leonard, and L. Magness. U.S. Army Research Laboratory. Test data. 1995.

Frank, K., and R. F. McLaughlin. "On the Overall Ballistic Performance of Tubular and Non-tubular Kinetic Energy Projectiles." BRL-TR-02100, U.S. Army Ballistic Research Laboratory, Aberdeen Proving Ground, MD, 1978.

Franzen, R. R. "Notes on Tubular Hypervelocity Penetrators." Proceedings of the Tenth International Symposium on Ballistics, San Diego, CA, 1987.

Franzen, R. R., and P. N. Schneidewind. "Observations Concerning the Penetration Mechanics of Tubular Hypervelocity Penetrators." International Journal of Impact Engineering, vol. 11, no. 3, pp. 289–304, 1991.

Hough, G. R. "Hydrocode Analysis of Tubular Kinetic Energy Penetrators." AFATL-TR-82-85, December 1982.

Keele, M. U.S. Army Ballistic Research Laboratory. Test data. 1992.

Kimsey, K. D. "Numerical Analysis of a Reduced-Mass Penetrator Concept." ARL report in preparation, 1995.

Littlefield, D. L., C. E. Anderson, Jr., Y. Partom, and S. J. Bless. "The Effects of Radial Confinement on Penetration Efficiency in RHA Targets." Draft preprint for presentation to the International Ballistics Symposium, Jerusalem, Israel, 1995.

Payne, J. J. "Impact Lethality of Long Hollow Cylinders." AEDC-TR-68-85, 1968.

Perciballi, J. W. U.S. Army Ballistic Research Laboratory. Test data. 1992.

Poston, R. Teledyne Firth Sterling Material Certification for TFS Order Number 953524, October 1990.

Pridgeon, Lori. U.S. Army Research Laboratory, Aberdeen Proving Ground, MD. Private communication. 16 March 1995.

Rapacki, E. J., K. Frank, R. B. Leavy, M. J. Keele, and J. Prifti. "Armor Steel Hardness Influence on Kinetic Energy Penetration." Preprint for presentation at the 15th International Symposium on Ballistics, Jerusalem, Israel, May 1995.

Sanders, E. J. "Lethality of Long Hollow Cylinders Impacting Normal and Oblique Targets." AEDC-TR-70-237, 1970.

Silsby, G. F. "High-Mass Launch Capability Development for the Army Research Laboratory's 50-mm High Pressure Powder Gun (Range 309A)." U.S. Army Research Laboratory, Aberdeen Proving Ground, MD, report in preparation, 1995.

Sorensen, B. R., K. D. Kimsey, G. F. Silsby, D. R. Scheffler, T. M. Sherrick, W. S. de Rosset, and K. Frank. "High Velocity Penetration of Steel Targets." Proceedings of the 1989 Hypervelocity Impact Symposium, San Antonio, TX, December 1989, and published in International Journal of Impact Engineering.

Zook, J., and K. Frank. U.S. Army Research Laboratory, Aberdeen Proving Ground, MD. Personal communication. June 1991.

APPENDIX A:

HYPERVELOCITY PENETRATION DATABASE

INTENTIONALLY LEFT BLANK.

Table A-1. Database and Notes

@DIR_PENETRATION@DIR_RHA_BY_WA@TBL_RODS_FAIR_CUM_89

0 ROW NO.	ENTRY SEQ.	1 STRIKING VELOCITY (km/s)	2 UNIT PEN. (P/L)	6 SOURCE TABLE tbl_rods_
1	22	0.527	0.042	_HandS_D17_6_10
2	23	0.642	0.066	_HandS_D17_6_10
3	77	0.665	0.063	_TATE_12
4	24	0.685	0.090	_HandS_D17_6_10
5	70	0.745	0.088	_TATE_12
6	84	0.785	0.128	_TATE_12
7	78	0.805	0.140	_TATE_12
8	71	0.885	0.168	_TATE_12
9	85	0.890	0.172	_TATE_12
10	86	0.940	0.239	_TATE_12
11	25	0.994	0.392	_HandS_D17_6_10
12	79	1.025	0.266	_TATE_12
13	26	1.036	0.398	_HandS_D17_6_10
14	87	1.060	0.345	_TATE_12
15	72	1.070	0.326	_TATE_12
16	80	1.075	0.343	_TATE_12
17	27	1.079	0.461	_HandS_D17_6_10
18	89	1.155	0.423	_TATE_12
19	73	1.180	0.441	_TATE_12
20	28	1.194	0.567	_HandS_D17_6_10
21	74	1.275	0.547	_TATE_12
22	14	1.291	0.513	_GFS_83
23	29	1.309	0.696	_HandS_D17_6_10
24	81	1.360	0.630	_TATE_12
25	30	1.382	0.754	_HandS_D17_6_10
26	82	1.445	0.735	_TATE_12
27	75	1.470	0.758	_TATE_12
28	13	1.494	0.719	_GFS_83
29	100	1.500	0.930	_BJERKE_89
30	31	1.509	0.908	_HandS_D17_6_10
31	17	1.520	0.848	_MAGNESS_mat
32	83	1.530	0.938	_TATE_12
33	18	1.533	0.863	_MAGNESS_mat
34	32	1.533	0.929	_HandS_D17_6_10
35	76	1.535	0.829	_TATE_12
36	16	1.551	0.839	_MAGNESS_mat
37	15	1.567	0.990	_MAGNESS_mat
38	33	1.588	0.971	_HandS_D17_6_10
39	99	1.600	1.020	_BJERKE_89
40	34	1.648	1.028	_HandS_D17_6_10
41	98	1.655	1.120	_BJERKE_89
42	35	1.752	1.113	_HandS_D17_6_10
43	36	1.830	1.185	_HandS_D17_6_10
44	1	1.865	1.119	_GFS_83
45	37	1.879	1.200	_HandS_D17_6_10
46	96	1.900	1.232	_SORENSEN_88
47	39	1.915	1.266	_HandS_D17_6_10
48	38	1.927	1.197	_HandS_D17_6_10
49	40	1.939	1.236	_HandS_D17_6_10
50	41	1.994	1.266	_HandS_D17_6_10

Table A-1. Database and Notes (continued)

@DIR_PENETRATION@DIR_RHA_BY_WA@TBL_RODS_FAIR_CUM_89 (Cont.)

0 ROW NO.	ENTRY SEQ.	1 STRIKING VELOCITY (km/s)	2 UNIT PEN. (P/L)	6 SOURCE TABLE tbl_rods_
51	97	2.040	1.293	_SORENSEN_88
52	89	2.050	1.274	_SORENSEN_88
53	95	2.060	1.279	_SORENSEN_88
54	42	2.061	1.293	_HandS_D17_6_10
55	90	2.070	1.263	_SORENSEN_88
56	43	2.073	1.315	_HandS_D17_6_10
57	44	2.109	1.296	_HandS_D17_6_10
58	92	2.120	1.297	_SORENSEN_88
59	69	2.140	1.317	_GFS_88_fair
60	45	2.152	1.315	_HandS_D17_6_10
61	66	2.180	1.306	_GFS_88_fair
62	91	2.220	1.373	_SORENSEN_88
63	46	2.224	1.345	_HandS_D17_6_10
64	19	2.250	1.304	_CUADROS_DSO
65	93	2.250	1.403	_SORENSEN_88
66	94	2.280	1.400	_SORENSEN_88
67	68	2.330	1.412	_GFS_88_fair
68	9	2.365	1.356	_GFS_83
69	8	2.409	1.415	_GFS_83
70	65	2.420	1.498	_GFS_88_fair
71	47	2.448	1.438	_HandS_D17_6_10
72	48	2.606	1.471	_HandS_D17_6_10
73	3	2.653	1.466	_GFS_83
74	49	2.715	1.480	_HandS_D17_6_10
75	2	2.742	1.463	_GFS_83
76	11	2.746	1.448	_GFS_83
77	50	2.788	1.486	_HandS_D17_6_10
78	51	2.848	1.468	_HandS_D17_6_10
79	58	2.890	1.520	_GFS_88_fair
80	59	2.900	1.459	_GFS_88_fair
81	20	2.910	1.500	_CUADROS_DSO
82	57	2.960	1.529	_GFS_88_fair
83	61	2.980	1.511	_GFS_88_fair
84	63	2.980	1.505	_GFS_88_fair
85	52	2.982	1.480	_HandS_D17_6_10
86	62	2.990	1.504	_GFS_88_fair
87	60	3.020	1.471	_GFS_88_fair
88	64	3.020	1.505	_GFS_88_fair
89	67	3.050	1.496	_GFS_88_fair
90	6	3.335	1.524	_GFS_83
91	7	3.449	1.550	_GFS_83
92	53	3.467	1.559	_HandS_D17_6_9
93	10	3.580	1.549	_GFS_83
94	54	3.709	1.553	_HandS_D17_6_9
95	21	3.730	1.640	_CUADROS_DSO
96	55	3.939	1.604	_HandS_D17_6_9
97	56	4.008	1.552	_GFS_88_fair
98	5	4.398	1.586	_GFS_83
99	4	4.415	1.592	_GFS_83
100	12	4.525	1.591	_GFS_83

Table A-1. Database and Notes (continued)

@DIR_PENETRATION@DIR_RHA_BY_WA@TBL_RODS_FAIR_CUM_89 (Cont.)

NOTES:

1. Table is provided without any warranty, express or implied. All data are unclassified, unlimited distribution. Notify me of any errors at gsilsby@tbd2.arl.mil or 410-278-6012 or FAX 410-278-6564. Graham Silsby, LMB, TED, WTD, ARL.

2. To firm up the final trend in various fits, the highest three velocity data points were weighted by a factor of three.

3. Data in tables ..._HandS_... are data of Hohler and Stilp digitized from graphs in various sources. This data is available in Anderson, Morris, and Littlefield [Jan 92], although the L/D 9 data in the cited reference differs from that digitized and the cited reference includes one apparant outlier excluded from the graphs.

4. Data in tables ..._TATE_... are data of Tate et al and are available in Anderson... [op. cit.].

5. Data in table ...GFS_83 are data of Silsby for 46 and 98 gram L/D 23 Kennametal W10 fully threaded rods attacking 6" and 8" wide RHA bar targets HBN 269, reported in the 8th Intl. Symp. Ball. and are available in Anderson... [op. cit.].

6. Data in table ..._SORENSEN_88 are data of Sorensen for 1 and 2 kg L/D 20 TFS X27 rods attacking stacks of 6" RHA HBN 269 2' square, reported in an unclassified paper entitled "High Velocity Penetration of Steel Targets," by Sorensen, Kimsey, Silsby, Scheffler, Sherrick, and de Rosset in the classified session of the 1989 Hypervelocity Impact Symposium and are available in Anderson... [op. cit.].

7. Data in table ..._GFS_88_fair are data of Silsby by AEDC VKF G-range personnel for 125 and 250 gram L/D 15, 20 and 30 TFS X27 rods attacking stacks of 3" RHA retempered to HBN 269, 1' square, reported in an unclassified paper entitled "High Velocity Penetration of Steel Targets," by Sorensen, Kimsey, Silsby, Scheffler, Sherrick, and de Rosset (as well as AEDC VKF G Range data reports) in the classified session of the 1989 Hypervelocity Impact Symposium and are available in Anderson... [op. cit.].

8. Data in table ..._Bjerke_89 are data from ARL's Bjerke, private communication, 1989.

9. Data in table ..._MAGNESS_mat are data from ARL's Magness and associates from appropriate parts of thier Materials Program, private communication, 1989.

10. Data in table ..._CUADROS_DSO are from 800 and 900 gram long rod shots for Jaimie Cuadros of the General Dynamics Valley Systems Division at GM's Delco Santa Barbara Operations two-stage light gas gun, private communication, 1984.

INTENTIONALLY LEFT BLANK.

APPENDIX B:

ARL RANGE 309A X21C ROLLED HOMOGENEOUS ARMOR NORMAL-INCIDENCE PENETRATION DATABASE

INTENTIONALLY LEFT BLANK.

Table B-1. Data Tabulation and Notes

@DIR_R309A@TBL_HROD_1
TFS X21C RODS vs SEMI-INFINITE RHA AT NORMAL INCIDENCE
FROM RANGE 309A TERMINAL BALLISTIC DATA BASE THRU 1994

0 LINE NO.	R309A SHOT NO.	1 PROJECT ENGINEER	2 DATA SET TYPE	3 ATYPICAL DATUM TYPE	4 ATYPICAL DATUM DISPOSITION	5 PENETRATOR TYPE	6 PENET. MASS (grams)	7 PEN. LENGTH (mm)	8 PEN. DIAM. (mm)
1	167	SILSBY	TGT:LAM/AIR	D=18, P LOW	RETAIN	L/D 1 WA	81.50	17.91	17.96
2	158	SILSBY	TGT:LAM/AIR	D=18		L/D 1 WA	78.90	17.50	19.06
3	157	SILSBY	TGT:LAM/AIR	D=18		L/D 1 WA	79.70	17.78	18.01
4	166	SILSBY	TGT:LAM/AIR	D=18		L/D 1 WA	81.50	18.06	18.06
5									
6	744	SILSBY	L/D 2			L/D 2 222g WA	223.00	39.98	19.94
7	745	SILSBY	L/D 2			L/D 2 222g WA	223.00	39.98	19.94
8									
9	729	SILSBY	L/D 3			L/D 3 333g WA	334.00	59.80	19.97
10	730	SILSBY	L/D 3			L/D 3 333g WA	332.60	59.83	19.96
11	502	SILSBY	L/D 3	D=19		L/D 3 287g WA	287.35	56.62	19.10
12									
13	499	SILSBY	SCALED D, M	D=19		L/D 4 386g WA	386.17	76.25	19.15
14	506	SILSBY	SCALED D, M	D=19		L/D 4 386g WA	385.75	76.20	19.05
15	512	BJERKE	SCALED D, M	D=19		L/D 4 386g WA	385.17	76.76	19.05
16	515	BJERKE	SCALED D, M	D=19		L/D 4 386g WA	385.22	76.05	19.05
17	361	PERCIBALLI	SAME D, M			L/D 4 444g WA	446.15	80.24	19.99
18	500	SILSBY	SCALED D, M	D=19		L/D 4 386g WA	389.43	76.23	19.15
19	746	SILSBY	SAME D, M			L/D 4 444g WA	446.00	79.98	19.89
20	501	SILSBY	SCALED D, M	D=19		L/D 4 386g WA	388.30	76.28	19.13
21	360	PERCIBALLI	TGT:LAM/AIR	L/D 4		L/D 4 444g WA	443.18	79.65	19.99
22									
23	268	SILSBY	L=100, SAME D			L/D 5 555g WA	556.61	100.00	20.00
24	267	SILSBY	L=100, SAME D			L/D 5 555g WA	556.61	100.02	20.00
25	261	KEELE	L=100, SAME D	LAM/HARDER	DISRGD, HARD	L/D 5 555g WA	557.79	100.03	20.00
26	269	SILSBY	L=100, SAME D			L/D 5 555g WA	557.33	100.15	20.01
27	249	SILSBY	L=100, SAME D			L/D 5 555g WA	557.40	100.03	20.00
28	248	SILSBY	L=100, SAME D			L/D 5 555g WA	556.60	100.07	20.00
29									
30	274	SILSBY	L=100, SAME M	D=17.78		H-ROD EQ DIA	439.45	100.03	17.78
31	276	SILSBY	L=100, SAME M	D=17.78		H-ROD EQ DIA	440.96	100.03	17.78
32	275	SILSBY	L=100, SAME M	D=17.78	DISRGD, YAW	H-ROD EQ DIA	441.61	100.03	17.81
33									
34	747	SILSBY	L=100 CORE	D=9.78		H-ROD CORE	133.03	99.95	9.78
35									
36	273	SILSBY	L=100 H-ROD			H-ROD (SEE C271)	438.04	100.14	20.00
37	272	SILSBY	L=100 H-ROD			H-ROD	437.97	100.03	19.99
38	737	SILSBY	L=100 H-ROD			H-ROD	444.00	100.00	20.00
39	271	SILSBY	L=100 H-ROD			H-ROD	437.48	100.06	19.99

Table B-1. Data Tabulation and Notes (continued)

@DIR_R309A@TBL_HROD_1 (Cont.)

0 LINE NO.	R309A SHOT NO.	9 PEN. L/D	10 STRIK. VELOC. (m/s)	11 TOTAL PENE-TRATION	12 TGT. 1 T/L	13 TGT. 1 T/D	14 WTD. TGT. HARDNESS (HBN)	15 TGT. Wmn./ DIAM.	16 TE1 PEN./ DIAM.	17 GROSS PEN./ DIAM.	18 P/L
1	167	1.00	1604	27.2	8.43	8.41	269	8.35	1.51	1.51	1.519
2	158	0.97	2083	36.6	9.16	8.41	286	8.41	2.03	2.03	2.206
3	157	0.99	2205	45.2	8.55	8.44	241	8.44	2.51	2.51	2.542
4	166	1.00	2458	47.0	8.31	8.31	269	8.31	2.60	2.60	2.603
5											
6	744	2.00	1548	63.5	3.80	7.62	269	7.52	3.18	3.18	1.590
7	745	2.01	1746	66.0	3.80	7.62	269	7.52	3.31	3.31	1.650
8											
9	729	2.99	1023	45.0	2.55	7.63	269	7.51	2.25	2.25	0.858
10	730	3.00	1497	85.0	2.55	7.63	269	7.51	4.26	4.26	1.442
11	502	2.96	1752	90.4	2.67	7.92	269	10.99	4.73	4.73	1.597
12											
13	499	3.98	1368	84.8	1.96	7.79	269	10.44	4.43	4.43	1.113
14	506	4.00	1497	96.5	1.97	7.88	269	10.66	5.07	5.07	1.267
15	512	3.98	1501	94.0	1.95	7.87	260	10.66	4.94	4.94	1.241
16	515	3.99	1509	95.4	1.97	7.87	260	10.66	5.01	5.01	1.254
17	361	4.01	1587	105.0	1.86	7.48	269	10.01	4.20	4.20	1.309
18	500	3.98	1637	103.7	1.96	7.79	262	9.97	5.41	5.41	1.360
19	746	4.02	1651	113.0	1.90	7.64	269	7.54	5.68	5.68	1.410
20	501	3.97	1684	111.8	1.97	7.85	269	10.98	5.84	5.84	1.465
21	360	3.98	1702	122.0	1.86	7.55	262	10.01	4.85	4.85	1.532
22											
23	268	5.00	1176	83.3	1.50	7.50	269	7.50	4.17	4.17	0.833
24	267	5.00	1195	89.3	1.51	7.55	269	7.50	4.46	4.46	0.893
25	261	5.00	1399	101.0	0.64	3.22	302	11.50	3.21	5.05	1.010
26	269	5.00	1412	112.5	1.51	7.57	269	7.50	5.62	5.62	1.124
27	249	5.00	1519	132.0	1.51	7.55	255	7.50	6.60	6.60	1.320
28	248	5.00	1588	137.0	1.51	7.54	269	7.50	6.85	6.85	1.369
29											
30	274	5.63	1540	121.0	1.50	8.45	269	11.25	6.81	6.81	1.210
31	276	5.63	1573	121.0	1.52	8.55	269	11.25	6.81	6.81	1.210
32	275	5.62	1582	99.0	1.51	8.51	273	11.23	5.56	5.56	0.990
33											
34	747	10.22	1485	89.7	1.52	15.54	269	15.34	9.17	9.17	0.897
35											
36	273	5.01	1545	106.0	1.49	7.45	269	10.00	5.30	5.30	1.059
37	272	5.00	1640	124.0	1.49	7.45	255	10.01	6.20	6.20	1.240
38	737	5.00	1648	137.0	1.52	7.62	269	7.50	6.85	6.85	1.370
39	271	5.01	1690	118.0	1.55	7.78	269	14.51	5.90	5.90	1.179

Table B-1. Data Tabulation and Notes (continued)

@DIR_R309A@TBL_HROD_1 (Cont.)

0 LINE NO.	R309A SHOT NO.	19 EXCESS P/L FACTOR	20 BULGE HEIGHT/ DIAM.	21 BULGE STRAIN CODE	22 TGT. REM. WEB/D.	23 MX. LAT. BULGE/ DIAM.	24 MN. LAT. WEB/DIA. (mm)	25 YAW/ CRIT. YAW	26 OTHER CON- FOUNDING EFFECTS
1	167	1.574	0.00	UC	6.89	0.06	3.06	0.00	PP STRIKE
2	158	1.680	0.00	UC	5.98	0.06	2.66	0.00	PP STRIKE
3	157	1.872	0.00	UC	5.93	0.00	2.39	0.00	NONE
4	166	1.832	0.00	UC	5.70	0.11	2.77	0.23	PP STRIKE
5									
6	744	1.761	0.00	UC	4.46	0.10	2.11	0.09	NONE
7	745	1.496	0.03	RI	4.31	0.05	2.71	0.07	NONE
8									
9	729	2.757	0.00	UC	5.06	0.05	2.50	0.34	NONE
10	730	1.709	0.00	UC	3.26	0.13	2.40	0.14	NONE
11	502	1.442	0.05	FB	3.09	0.00	3.40	0.17	PP STRUCK IN CHANNEL
12									
13	499	1.621	0.10	FB	3.38	0.00	3.86	0.41	NONE
14	506	1.502	0.10	FB	2.78	0.00	3.20	0.45	NONE
15	512	1.463	0.05	FB	2.99	0.00	4.20	0.41	NONE
16	515	1.462	0.05	FB	2.92	0.00	4.20	0.07	NONE
17	361	1.383	0.10	FB	1.75	0.10	3.70	0.42	PP STRIKE
18	500	1.361	0.10	FB	2.47	0.00	4.18	0.33	NONE
19	746	1.391	0.15	FB	1.87	0.15	2.51	0.47	NONE
20	501	1.400	0.10	FB	1.99	0.00	3.40	0.55	NONE
21	360	1.441	0.30	RO	1.30	0.15	3.75	0.19	NONE
22									
23	268	1.809	0.00	UC	3.40	0.05	2.50	0.66	PL PRECRKED MIDPL, PP
24	267	1.855	0.05	FB	3.10	0.10	2.35	0.71	NONE
25	261	1.393	0.15	FB	1.55	0.00	2.10	0.84	HARDER, LAMINATED TGT
26	269	1.517	0.02	RI	1.90	0.25	1.95	0.14	NONE
27	249	1.518	0.15	FB	0.90	0.25	2.15	1.05	PP STRIKE
28	248	1.445	0.15	FB	0.55	0.40	2.05	1.04	PP STRIKE
29									
30	274	1.354	0.17	FB	1.91	0.11	3.94	1.12	NONE
31	276	1.300	0.17	FB	1.63	0.17	4.22	0.17	NONE
32	275	1.052	0.08	FB	2.92	0.11	3.93	2.54	DISREGARD, HI YAW
33									
34	747	1.082	0.00	UC	6.24	0.00	5.62	1.69	HI YAW (KEYHOLE)
35									
36	273	1.177	0.15	FB	2.20	0.00	3.55	0.99	NONE
37	272	1.237	0.10	FB	1.40	0.05	3.50	0.41	NONE
38	737	1.356	0.25	FB	0.65	0.10	3.00	0.00	NONE
39	271	1.121	0.15	FB	1.80	0.10	4.25	0.24	NONE

Table B-1. Data Tabulation and Notes (continued)

@DIR_R309A@TBL_HROD_1 (Cont.)

0 LINE NO.	R309A SHOT NO.	27 P. PL. DAMAGE MEAS.	28 ROD O/A RECOV. L/D	29 ROD ERODED L/D	30 COMMENTS
1	167	17	0.0	1.00	5.54g PUSHER SPLAT RECOVERED
2	158	6	0.0	0.97	
3	157	0	0.0	0.99	
4	166	19	0.0	1.00	PEN ADJUSTED F/ PP HIT
5					
6	744	0	0.5	1.51	BASE CRACKED IN QUARTERS
7	745	0	0.3	1.70	BASE BROKEN INTO CENTRAL
8					
9	729	0	1.3	1.72	PETALS JUST STARTING TO TURN BACK
10	730	0	0.9	2.10	PETALS NEARLY FULLY TURNED BACK
11	502	36	0.4	2.52	ROD BASE A SPLAT ONLY
12					
13	499	0	0.9	3.04	ENTR DIA DISTORTED
14	506	0	1.0	3.04	1st TIPPER PL SHOT
15	512	0	1.0	3.07	DATA: BJERKE RPT ARL-MR-51
16	515	0	1.0	3.04	DATA: BJERKE RPT ARL-MR-51
17	361	76	0.6	3.46	
18	500	72	0.8	3.17	
19	746	0	0.5	3.52	BASE LODGED YAWED 30 DEG
20	501	72	0.7	3.26	BASE SL DEFORM BY PP STRIKE
21	360	152	0.7	3.33	
22					
23	268	51	1.2	3.80	CHECK PEN. C268.
24	267	0	1.2	3.85	
25	261	76	1.1	3.94	5 g KERN? RECOV PRESSED INTO SIDE OF CH BOTTOM
26	269	0	1.2	3.80	CHECK PEN. C269.
27	249	413	1.1	3.95	
28	248	127	0.0	5.00	CHECK PEN. THIN WEB.
29					
30	274	0	1.0	4.67	
31	276	0	1.0	4.61	
32	275	0	1.5	4.10	HI YAW DISREGARD
33					
34	747	0	1.2	9.05	CH CURVES AWAY FM TAIL GOUGE
35					
36	273	77	0.0	5.01	H-ROD
37	272	102	0.0	5.00	H-ROD
38	737	0	0.0	5.00	H-ROD
39	271	51	0.0	5.01	H-ROD

Table B-1. Data Tabulation and Notes (continued)

@DIR_R309A@TBL_HROD_1 (Cont.)

NOTES:

1. TBL_HROD_1 contains all R309A data on Teledyne Firth Sterling X21C rods swaged 25% by the large bar process and aged at 500C, versus semi-infinite rolled homogeneous armor nominally Brinnel 269 (HBN 269) at normal incidence. Current through 1994.
2. The number of target plates unpenetrated is a measure of axial inertial confinement. A value of 0 was assigned for air, 1 for a thinner plate, 2 for a thicker plate, and 3 for the butt.
3. A number of judgement calls have been used to maximize the utility of the data set.
   a. The unknown recovered rod length on shot 506 was set as the average from two similar shots, 512 and 515.
   b. A remaining web thickness value of the target thickness less the penetration depth has been assigned in shots where this datum has not been measured.
   c. A lateral bulge height of 0 has been assigned for the unknown values for shots 157 and 261.
4. The PUSHER PLATE DAMAGE MEASURE is the product of the mass of the pusher plate times the fraction of pusher judged to have entered the penetration channel (hole) times either 1 for titanium or 2 for steel pusher plate times 0-3 for orientation (0 = missed, 1 = flat, 2 = inclined, and 3 = edge on).

COMMENTS:

SHOT 268: Check for consistency of penetration depth. Post-shot, target block nearly split in two by crack in the midplane (perpendicular to the shot line), with some corroded surfaces indicating that it was pre-cracked. Treat like laminated target?

SHOT 269: Check for consistency of penetration depth. Zone of unusual deep radial and transverse cracks originating at target lateral surface at the (thin) web.

SHOT 271-3 and 737: A holed-out rod (H-rod) is a 100 mm long by 20 mm diameter cylinder drilled thru with a pattern of eight equally spaced 3 mm diameter holes parallel to the axis on 13 inch diametral centers. The average penetration hole diameter is used for computing critical yaw.

- SHOT 271: Fluted hole, 41 mm minor diameter, 48 mm major diameter, axis inclined to shot line.
- SHOT 272: Fluted hole, 42 mm minor diameter, 47 mm major diameter.
- SHOT 273: Fluted hole, 39 mm minor diameter, 43 mm major diameter, axis inclined.
- SHOT 737: Fluted hole, 43 mm minor diameter, 51 mm major diameter.

SHOTS 512 and 515: Target hardness arbitrarily assigned a value of HBN 260 based on published average values.

Table B-2. Detailed Explanation of Database Format

NOTES TO TABLE TBL_HROD_1, WHICH IS EXTRACTED FROM THE TERMINAL BALLISTIC LOG FOR RANGE 309A. (ALL SHOTS THRU 1994.)

1 PROJECT ENGINEER	2 DATA SET TYPE	3 ATYPICAL DATUM TYPE	4 ATYPICAL DATUM DISPOSITION	5 PENETRATOR TYPE	6 PENETRATOR MASS
	AIR - Target backed by air. D - Diameter. HHA - High-hard armor. INF - Semi-infinite ie very thick. L - Length. LAM - Laminated. RHA - Rolled Homogeneous Armor. TGT - Type of target assembly. @0 or @ whatever - Target obliquity.	HARDER - Target is significantly harder than HBN 269. P - Penetration.	DISRGD - Disregard the data from this shot.	H-ROD - 100 mm long by 20 mm diameter with 8 3.2 mm thru holes on 13 mm diameter circle. WA - Tungsten alloy.	

7 PENETRATOR LENGTH	8 PENETRATOR DIAMETER	9 PENETRATOR L/D	10 STRIKING VELOCITY	11 TOTAL PENETRATION	12 (TGT ELEMENT #1 NORMAL THICKNESS)/ (ROD LENGTH)	13 (TGT ELEMENT #1 NORMAL THICKNESS)/ (ROD DIAMETER)

14 WEIGHTED AVERAGE TARGET HARDNESS	15 (TGT. MIN.WIDTH)/ (ROD DIAMETER)	16 (TGT. EL. 1 PEN.)/ (ROD DIAMETER)	17 (GROSS PENETRATION)/ (ROD DIAMETER)	18 P/L
Computed as (sum of the products of the hardness times thickness or penetration depth of individual target elements) divided by the total normal penetration.				

Table B-2. Detailed Explanation of Database Format (continued)

NOTES TO TABLE TBL_HROD_1 (Cont.)

19 EXCESS P/L-FACTOR	20 (TGT. BULGE HEIGHT)/(ROD DIAMETER)	21 BULGE STRAIN CODE	22 (TGT. RE-MAINING WEB)/(ROD DIAM.)	23 (MAX. LATERAL BULGE)/(ROD DIAMETER)	24 (MIN. LAT. WEB)/(ROD DIAMETER)
Used in analysis only.		A measure of target rear surface strain: UC - Unchanged. RI - Rust intact. (Some change, but rust still clings. RO - Rust off in central zone. SC - (Mill) scale cracked. IC - Incipient cracks CR - Small cracks. OC - Open cracks. Append width in mm. TC - Thru cracks. SO - Scab off. SP - True spall off. FB - Flatted bulge: bulge stopped by target backer.			Web is thickness of material between channel wall and target edge. Use the distance from strike point to target edge if actual web not measured.

Table B-2. Detailed Explanation of Database Format (continued)

NOTES TO TABLE TBL_HROD_1 (Cont.)

25 (TOTAL YAW)/ (CRITICAL YAW)	26 OTHER CONFOUNDING EFFECTS	27 PUSHER PLATE DAMAGE MEASURE	28 ROD OVERALL RECOVERED L/D	29 ROD ERODED L/D	30 COMMENTS
Shot is judged acceptable for YAW/YAWcr < 1. Ycr = arcsin((H-D)/2L) Can be undefined for for very short rods. See reference.	MIDPL - Midplane, parallel to rolling plane. PL - Plate. PP - Pusher plate strike. PRECRKED - Pre-existing crack in plate.	See table notes.	L/D of recovered tail end of rod.	Ratio of rod material eroded to rod original length.	BASE ... - Tail-end of eroded rod. BASE CRACKED ... - When rod nearly eroded completely, the tail breaks into sectors. CH CURVES - Penetration channel curves. Sign of a high yaw hit. KERN - Cusped piece of penetrator/target material thought to sep-encompass the pen.-tgt. interface. PETALS ... - A measure of the inertial forces to which target face is subjected.

APPENDIX C:

ANALYSIS DETAILS

INTENTIONALLY LEFT BLANK.

Table C-1. Pooled Data Set of R309A and Farrand, With Notes

'SEMI-INFINITE' RHA NORMAL PENETRATION DATA,
X21C FLAT NOSE, FLAT BASE SHORT RIGHT CIRCULAR CYLINDERS AND
GTE VARIOUS HARDNESSES HEMI-NOSE, FLAT BASE LONG RCCS

LINE NO.	RANGE & SHOT NO.	PEN. HRD. (HRC)	PEN. L/D	STRIK. VELOC. (km/s)	MN. LAT. WEB/DIA. (mm)	P/L	RESID-UALS
1	R309A 167	47	1.00	1.604	3.06	1.519	-0.034
2	158	47	0.97	2.083	2.66	2.206	0.010
3	157	47	0.99	2.205	2.39	2.542	0.191
4	166	47	1.00	2.458	2.77	2.603	0.257
5							
6	R309A 744	47	2.00	1.548	2.11	1.590	-0.004
7	745	47	2.01	1.746	2.71	1.650	-0.128
8							
9	R309A 729	47	2.99	1.023	2.50	0.858	0.359
10	730	47	3.00	1.497	2.40	1.442	0.070
11	502	47	2.96	1.752	3.40	1.597	-0.048
12							
13	R309A 499	47	3.98	1.368	3.86	1.113	0.145
14	506	47	4.00	1.497	3.20	1.267	0.037
15	512	47	3.98	1.501	4.20	1.241	0.059
16	515	47	3.99	1.509	4.20	1.254	0.059
17	361	47	4.01	1.587	3.70	1.309	-0.033
18	500	47	3.98	1.637	4.18	1.360	-0.033
19	746	47	4.02	1.651	2.51	1.410	-0.166
20	501	47	3.97	1.684	3.40	1.465	-0.043
21	360	47	3.98	1.702	3.75	1.532	0.026
22							
23	R309A 268	47	5.00	1.176	2.50	0.833	0.136
24	267	47	5.00	1.195	2.35	0.893	0.148
25	261	47	5.00	1.399	2.10	1.010	-0.163
26	269	47	5.00	1.412	1.95	1.124	-0.117
27	249	47	5.00	1.519	2.15	1.320	-0.073
28	248	47	5.00	1.588	2.05	1.369	-0.181
29							
30	R309A 274	47	5.63	1.540	3.94	1.210	0.012
31	276	47	5.63	1.573	4.22	1.210	-0.026
32	275	47	5.62	1.582	3.93	0.990	-0.272
33							
34	R309A 747	47	10.22	1.485	5.62	0.897	-0.045
35							
36	R110E 4034	39	9.83	1.473	9.60	0.900	-0.012
37	Rc 39 4035	39	9.83	1.463	9.60	0.870	-0.028
38	GTE 4036	39	9.83	1.477	9.60	0.840	-0.077
39	4037	39	9.83	1.477	9.60	0.900	-0.017
40	4038	39	9.83	1.479	9.60	0.850	-0.070
41	4039	39	9.83	1.475	9.60	0.880	-0.035
42	4040	39	9.83	1.459	9.60	0.860	-0.033
43							
44	R110E 3981	39	14.83	1.651	11.00	0.950	-0.048
45	Rc 39 3976	39	14.83	1.838	11.00	1.190	0.032
46	GTE 3982	39	14.83	1.839	11.00		
47	3981	39	14.83	1.944	11.00	1.230	0.004
48	3984	39	14.83	1.995	11.00	1.250	-0.003
49							

Table C-1. Pooled Data Set of R309A and Farrand, With Notes (continued)

LINE NO.	RANGE & SHOT NO.	PEN. HRD. (HRC)	PEN. L/D	STRIK. VELOC. (km/s)	MN. LAT. WEB/DIA. (mm)	P/L	RESID-UALS
50	R110E 3124	39	19.83	1.169	12.12	0.430	0.027
51	Rc 39 3125	39	19.83	1.331	12.12	0.570	-6e-04
52	GTE 3126	39	19.83	1.484	12.12	0.740	0.003
53	3127	39	19.83	1.573	12.12	0.850	0.022
54							
55	R110E 2493	39	24.83	1.078	13.06	0.300	-2e-04
56	Rc 39 2494	39	24.83	1.315	13.06	0.560	0.042
57	GTE 2495	39	24.83	1.498	13.06	0.760	0.057
58	2496	39	24.83	1.626	13.06	0.890	0.068
59							
60	R110E 2705	41	9.83	1.596	9.60	0.990	-0.080
61	Rc 41 2706	41	9.83	1.297	9.60	0.660	-0.011
62	GTE						
63							
64	R110E 2563	41	29.83	1.077	13.88	0.270	-0.022
65	Rc 41 2566	41	29.83	1.097	13.88	0.280	-0.028
66	GTE 2564	41	29.83	1.286	13.88	0.520	0.043
67	2567	41	29.83	1.312	13.88	0.540	0.038
68	2565	41	29.83	1.504	13.88	0.750	0.058
69	2569	41	29.83	1.536	13.88	0.770	0.048
70	2568	41	29.83	1.598	13.88	0.810	0.032
71							
72	R110E 1974	44	9.83	1.079	9.60	0.450	0.045
73	Rc 44 2037	44	9.83	1.102	9.60	0.480	0.051
74	GTE 2038	44	9.83	1.286	9.60	0.710	0.053
75	1975	44	9.83	1.298	9.60	0.690	0.017
76	2039	44	9.83	1.499	9.60	0.940	-0.007
77	1976	44	9.83	1.527	9.60	0.970	-0.013
78	2040	44	9.83	1.696	9.60	1.130	-0.053
79							
80	R110E 1978	44	14.83	1.086	11.00	0.380	0.017
81	Rc 44 2041	44	14.83	1.097	11.00	0.400	0.027
82	GTE 1979	44	14.83	1.291	11.00	0.590	0.006
83	2042	44	14.83	1.297	11.00	0.640	0.049
84	1980	44	14.83	1.500	11.00	0.810	-0.024
85	1981	44	14.83	1.682	11.00	1.040	0.012

Table C-1. Pooled Data Set of R309A and Farrand, With Notes (continued)

NOTES:

1. TBL_17_6_MULT is from TBL_HROD_1, with extraneous data deleted, and R110E high L/D data of Farrand added, seeking the influence of target extent and closeness to the nearest edge on penetration depth while fitting P/L vs V vs L/D. It contains all R309A data on Teledyne Firth Sterling X21C rods swaged 15% by the large bar process and aged at 500 C for 1 hr, vs semi-infinite rolled homogeneous armor nominally Brinnel 269 (HBN 269) at normal incidence. R309A data is complete through 1994.

2. A number of judgement calls have been used to maximize the utility of the data set.

3. A lateral web thickness of W/2, W the target minimum lateral dimension, has been assigned in shots where this datum has not been measured.

4. R110E data has been used to provide sufficient long-rod penetrator data with large lateral webs that the fitting functions will have a credible baseline. The rods were of slightly different composition and processing than the X21C short rods for which the fit is sought, but because their density is 17.6 g/cm^3 and their strengths are similar, their semi-infinite RHA penetration depths should be comparable. They were shot into one or two 6" cubes of RHA (nominally HBN 269) with air behind. Nothing can be done to account for the difference in axial constraint, although this effect is thought to be small. The L/D was adjusted down by 1/6 to account for the hemispherical nose, and nominal diameters were computed from the nominal mass and density.

5. After trying various forms suggested by examination of the effects of individual factors on various data sets, the following multiple regression yielded the best fit (SD = 0.094, 69 data, coefficients highly correlated):

   P/L = (0.940 + 0.000893*(30-[L/D])^2)*(0.852 + 0.960/([WEB/D]^2))*(f(V)),
   where f(V) = (1.236+0.0875*V)/(1+117*exp((-3.5)*V)).

   To eliminate the correlation, the 0.940 and 0.960 terms were arbitrarily set to 1.000 and the function refit, with SD = 0.093,

   P/L = (1 + 0.000906*(30-[L/D])^2)*(0.807 + 1/([WEB/D]^2))*(f(V)).

   In this form, the error minimum is rather tight around the two parameters, which have 95% confidence regions of 0.000767 < C1 < 0.001044 and 0.7593 < C2 < .8546. In settling on this form, the effect of rod hardness on this data set was found to be essentially zero and was suppressed. Using a power term in the web term of 1 rather than 2 increased the SD unacceptably.

6. On checking shot 268 to see if it should be treated like a laminated target, the residual on the above fit was +0.136. Post-shot, the target block was nearly split in two by a crack in the midplane (perpendicular to the shot line), with some corroded surfaces indicating that it was pre-cracked. The residual on shot 269 to the above fit was -0.117. Post-shot, the target displayed a thin web with large cracks. The two offsetting residuals suggest that this is unexplainable variation.

Table C-2. Fitting Parameters for Individual and Multiple Regression

'S' vs HARDNESS vs L/D
With Weighting Factors
(Number of Data)

SOURCE	HARD. (HRC)	L/D	INDIV. 'S'	NO. DATA	SD of FIT	MULT. FIT 'S'
DATA	39	10	1.0710	7	0.025	1.0710
DATA	39	15	0.9831	4	0.033	0.9768
DATA	39	20	0.9057	4	0.015	0.9096
DATA	39	25	0.8964	4	0.014	0.8692
DATA	41	10	1.0540	4	0.033	1.0833
DATA	41	30	0.8567	7	0.027	0.8681
DATA	44	10	1.1200	7	0.011	1.1018
DATA	44	15	0.9996	6	0.027	1.0077
MULT REGRESS FIT	47	30		0	0.019	0.9051

NOTES:

1. The tabulated 'Ss' are the constant factors obtained for the specific modified exponential fit to Farrand's P/L vs Velocity data for 17.6 g/cm^2 tungsten long rods vs 6" RHA cubes as follows:
   P/L = S*((1.236+0.0875*x)/(1+117*exp((-3.5)*x)))

2. Examination of the HRC 39 data suggests essentially no difference between using a 2nd order polynomial (parabolic) fit or a hyperbolic fit (A + B/(L/D)) fit in P/L vs L/D. The former was chosen because it provides a (perhaps too) rapid close on a lower bound on the function, good match in curvature in the region of the data, and a less steep slope beyond the data. Various parabolic fits were tried. The confidence regions on the parameters are sufficiently broad (the data scatter is large and the data scant) that arbitrarily setting the minimum at L/D = 30 (which probably makes some physical sense) and assuming no variation in the location of this minimum L/D with rod hardness should be adequate to model the data without distorting the sought-after result (to adjust the penetration to that of an HRC 47 rod alloy). Only three hardness were used in the test, so that at best a linear model in rod hardness is all that can be justified.

3. Thus, the model S = A*(f-30)**2 + B*h + C) was fit by multiple regression, with numbers weighted by the number of data used in obtaining the original fitted 'Ss'. S is the multiplier on the modified exponential form sought here, A, B, and C are fitting parameters, h is the rod hardness and f the L/D (fineness ratio). When curves generated by this function are compared with fits to individual data subsets, the results are essentially indistinguishable for all but two cases.

4. The final form is S = 0.000538*(f-30)^2 + (0.00617*h) + 0.615, SD = .019, multiple R^2 = 0.97. Examination of the confidence intervals on A and B reveal that A lies between about 0.00042 and 0.00066, (L/D is almost certainly a factor) and B lies between about -0.003 and +0.015, hence rod hardness may be only weakly coupled to penetration, if at all. The form is (arbitrarily) defined for 35 < HRC < 50 and 9 < L/D by setting L/D = 30 for all L/D > 30.

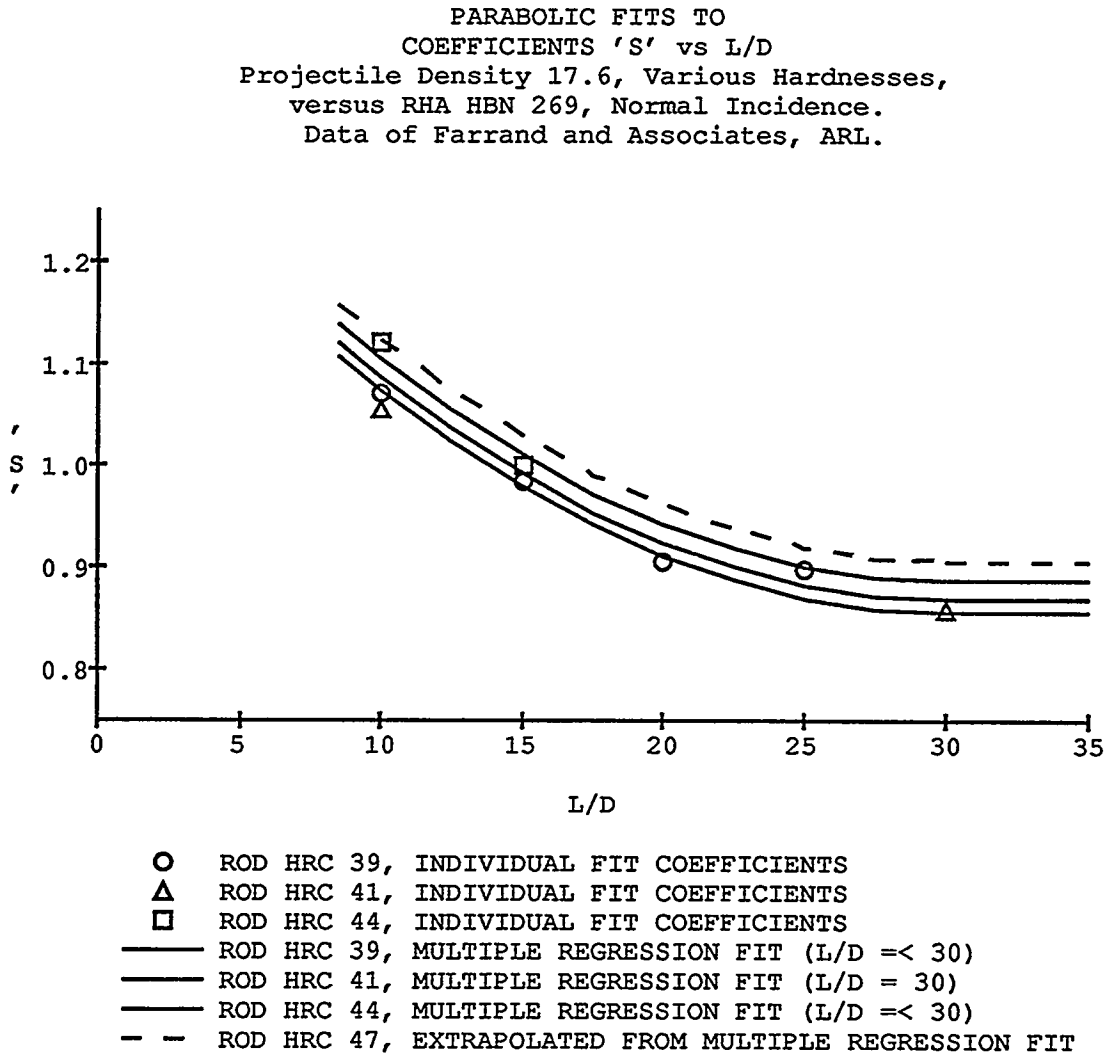

Figure C-1. Individual fits to data of Farrand fit by multiple regression.

INTENTIONALLY LEFT BLANK.

NO. OF COPIES	ORGANIZATION
2	DEFENSE TECHNICAL INFO CTR ATTN DTIC DDA 8725 JOHN J KINGMAN RD STE 0944 FT BELVOIR VA 22060-6218
1	DIRECTOR US ARMY RESEARCH LAB ATTN AMSRL OP SD TA 2800 POWDER MILL RD ADELPHI MD 20783-1145
3	DIRECTOR US ARMY RESEARCH LAB ATTN AMSRL OP SD TL 2800 POWDER MILL RD ADELPHI MD 20783-1145
1	DIRECTOR US ARMY RESEARCH LAB ATTN AMSRL OP SD TP 2800 POWDER MILL RD ADELPHI MD 20783-1145
	ABERDEEN PROVING GROUND
2	DIR USARL ATTN AMSRL OP AP L (305)

NO. OF COPIES	ORGANIZATION
1	CIA ATTN J BACKHOFEN NHB RM 4P07 WASHINGTON DC 20505
1	DEFENSE NUCLEAR AGENCY ATTN TECH LIBRARY 6801 TELEGRAPH RD ALEXANDRIA VA 22192
2	DARPA DIRECTOR LAND SYSTEMS OFFICE ATTN DR J RICHARDSON P KENNEY 3701 N FAIRFAX DR ARLINGTON VA 22203-1714
1	HQDA OUSD AT&E ATTN T JULIAN PENTAGON RM 3D1084 WASHINGTON DC 20310
1	HQDA ASMCO ATTN DAMO FDH J SUTTON PENTAGON RM 2D741 WASHINGTON DC 20310
1	COMMANDER USAMC ATTN AMCDRA R BLACK 5001 EISENHOWER AVE ALEXANDRIA VA 22333-0001
2	COMMANDER USA ARDEC ATTN AMSTA AR CC J HEDDERICH AMSTA AR TD V LINDER BLDG 1 PICATINNY ARSENAL NJ 07806-5000
1	COMMANDER USA ARDEC AMSTA AR INC TECH LIB BLDG 59 PICATINNY ARSENAL NJ 07806-5000

NO. OF COPIES	ORGANIZATION
1	COMMANDER USA ARDEC ATTN AMSTA AR LSI J BILLACK BLDG 62S PICATINNY ARSENAL NJ 07806-5000
3	COMMANDER USA ARDEC AMSTA AR CCH A M PALATHINGAL AMSTA AR CCL D T HUNG AMSTA AR CCL D W WILLIAMS BLDG 65N PICATINNY ARSENAL NJ 07806-5000
7	COMMANDER USA ARDEC ATTN AMSTA AR CCH J DELORENZO AMSTA AR CCH A R CARR AMSTA AR CCH A P CHRISTIAN AMSTA AR CCH A M CONNER AMSTA AR CCH A S MUSELLI AMSTA AR CCH B P VALENTI AMSTA AR CCH C M DANESI BLDG 65 S PICATINNY ARSENAL NJ 07806-5000
1	COMMANDER USA ARDEC ATTN AMSTA AR FS T GORA BLDG 94 PICATINNY ARSENAL NJ 07806-5000
1	COMMANDER USA ARDEC ATTN AMSTA AR FSP A T HARITOS BLDG 353N PICATINNY ARSENAL NJ 07806-5000
2	COMMANDER USA ARDEC ATTN AMSTA AR AET W EBIHARA AMSTA AR AET M S CYTRON BLDG 355 PICATINNY ARSENAL NJ 07806-5000

NO. OF COPIES	ORGANIZATION
1	COMMANDER USA ARDEC ATTN AMSTA AR FSE B KNUTELSKY BLDG 382 PICATINNY ARSENAL NJ 07806-5000
1	COMMANDER USA ARDEC ATTN AMSTA AR AET M D KAPOOR BLDG 1609 PICATINNY ARSENAL NJ 07806-5000
16	OPM TMAS ATTN SFAE ASM TMA COL A BREGARD SFAE ASM TMA C KIMKER SFAE ASM TMA AS R BILLINGTON SFAE ASM TMA AS B POTTER SFAE ASM TMA MS R BROWN SFAE ASM TMA MS P CARDELL SFAE ASM TMA MS K FEHSAL SFAE ASM TMA MS D GUZIEWICZ SFAE ASM TMA MS R JOINSON SFAE ASM TMA MS R KOWALSKI SFAE ASM TMA MS C ROLLER SFAE ASM TMA MS H YUEN SFAE ASM TMA RM J MCGREEN SFAE ASM TMA PA E KOPACZ SFAE ASM TMA PA R LINDSEY SFAE ASM TMA PA V ROSAMILIA BLDG 171A PICATINNY ARSENAL NJ 07806-5000
1	COMMANDER USA BELVOIR RD&E CTR ATTN STRBE NAN TECH LIBRARY FT BELVOIR VA 22060-5166
1	DIRECTOR USA BENET LABS ATTN SMCAR CCB DR C KITCHENS WATERVLIET NY 12189-4050
1	COMMANDER USA TACOM RD&E CENTER ATTN AMCPM ABMS SA J ROWE WARREN MI 48397-5000

NO. OF COPIES	ORGANIZATION
2	COMMANDER USA TACOM ATTN AMSTA RS J THOMPSON S GOODMAN WARREN MI 48397-5000
2	COMMANDER US ARMY TACOM ATTN SFAE ASM SS T T DEAN M RYZYI WARREN MI 48397-5000
3	LOSAT PROJECT OFFICE ATTN SFAE MSL LS EM R PALLADINO A DYKSTRA B SABOURIN REDSTONE ARSNL AL 35898-8051
1	DIRECTOR OF CMBT DEV USA ARMOR SCHL ATTN ATSB CD ML TB J BUTLER FT KNOX KY 40121-5215
1	COMMANDER USA MICOM ATTN AMSMI RD MR W MCCORKLE REDSTONE ARSNL AL 35898-5010
2	COMMANDER USA MICOM ATTN AMSMI RD ST WF M SCHEXNAYDER D LOVELACE REDSTONE ARSENAL AL 35898-5247
1	COMMANDER USA RESEARCH OFFICE ATTN K LYER MATERIAL SCIENCE DIV PO BOX 12211 RESEARCH TRIANGLE PARK NC 27709-2211

NO. OF COPIES	ORGANIZATION
2	COMMANDER USA NGIC ATTN S MINGLEDORF J MORGAN 220 7TH ST NE CHARLOTTESVILLE VA 22901
3	COMMANDER USA SPACE DEFNSE CMD ATTN CSSD KE E WILKINSON R CURTIS R BROWN PO BOX 1500 HUNTSVILLE AL 35807-3801
1	CH OF NAVAL RSRCH ATTN A J FAULSDITCH ONT 23 OFC OF NAVAL TECH BALLSTON TOWERS ARLINGTON VA 22217
1	DIRECTOR NAVAL CIVIL ENGR LAB ATTN J YOUNG CODE L 56 PORT HUENEME CA 93043
1	COMMANDER NSWC ATTN TECH LIBRARY CHINA LAKE CA 93555
4	COMMANDER NSWC ATTN J C MONOLO CODE G 34 M SHAMBLEN W HORT TECH LIBRARY DAHLGREN VA 22448-5000
4	COMMANDER NSWC ATTN R GARRETT R 12 J FOLTZ R 32 H DEJARNETTE R 32 TECH LIBRARY 10901 NEW HAMPSHIRE AVE SILVER SPRING MD 20903-5000

NO. OF COPIES	ORGANIZATION
1	NUSC NEWPORT ATTN S DICKINSON CODE 8214 NEWPORT RI 02841
1	COMMANDER NAVAL RSRCH LAB ATTN A WILLIAMS 4555 OVERLOOK SW WASHINGTON DC 20375
1	MSD ENL ATTN W DYESS EGLIN AFB FL 32542-5000
2	AIR FORCE WRIGHT LAB ATTN TECH LIBRARY DR J C FOSTER ARMAMENT DIVISION 101 EGLIN AVE STE 239 EGLIN AFB FL 32542
1	USMC MCRDAC PM ATTN D HAYWOOD GRNDS WPNS BR FIREPOWER DIV QUANTICO VA 22134
1	USMC PROG OFC DAVID TAYLOR RSRCH CTR ATTN W ZEITFUSS CODE 1240 BETHESDA MD 20084
1	US DEPT OF ENERGY OFC OF SCIENCE TECH INFO ATTN L WHITEHEAD PO BOX 62 OAK RIDGE TN 37831
3	LANL ATTN H SHEINBERG P DUNN B HOGAN LOS ALAMOS NM 87545
1	LANL ATTN D RABERN GROUP MEE 13 MS J576 LOS ALAMOS NM 87545

NO. OF COPIES	ORGANIZATION
1	LANL ATTN TECH LIB PO BOX 1663 LOS ALAMOS NM 87545
1	LANL ATTN J WALSH PO BOX 1663 LOS ALAMOS NM 87545
1	LANL ATTN L HULL M 8 PO BOX 1663 LOS ALAMOS NM 87545
1	LANL ATTN L HANTEL PO BOX 1663 LOS ALAMOS NM 87545
5	LLNL ATTN R GOGOLEWSKI L321 R YOUNG L282 M FINGER L011 C CLINE J REAUGH L321 PO BOX 808 LIVERMORE CA 94550
1	SANDIA NATIONAL LABS ATTN J ASAY DEPT 1430 ALBUQUERQUE NM 87185-5800
2	SANDIA NATIONAL LABS ATTN A ROBINSON R NELLUMS ALBUQUERQUE NM 87185-5800
2	SANDIA NATIONAL LABS ATTN D GRADY DEPT 1433 MS 0821 ALBUQUERQUE NM 87185-5800
3	BATTELLE PNW LAB ATTN B GURWELL G DUDDER R SHIPPELL PO BOX 999 RICHLAND WA 99352

NO. OF COPIES	ORGANIZATION
2	BATTELLE TWSTIAC ATTN L VESCILIUS 505 KING AVE COLUMBUS OH 43201
1	BATTELLE COLUMBUS LABS 505 KING AVE COLUMBUS OH 43201
1	BATTELLE EDGEWOOD OPNS OFC ATTN L HERR 2113 EMMORTON PARK RD EDGEWOOD MD 21040
3	NM TECH EMRTC ATTN D COLLIS J FORSTER M STANLEY CAMPUS STA SOCORRO NM 87801
5	INSTITUTE FOR ADV TECH ATTN DR T KIEHNE S BLESS R SUBRMANIAN D BARNETT M ERENGIL 40302 W BRAKER LN AUSTIN TX 78759-5329
5	SOUTHWEST RSRCH INST ATTN DR C ANDERSON J RIEGEL D LITTLEFIELD P COX J LANKFORD MGR BALLISTICS SCIENCE SECT PO BOX 28510 SAN ANTONIO TX 78228-0510
2	UNIV DAYTON RSRCH INST ATTN A PIEKUTOWSKI H SWIFT 300 COLLEGE PARK DAYTON OH 45469-0180

NO. OF COPIES	ORGANIZATION
1	UNIVERSITY OF ALABAMA ATTN S JONES DEPT ENG MECH PO BOX 820278 TUSCALOOSA AL 35487-0278
1	JOHNS HOPKINS UNIV DEPT MECH ENG ATTN K RAMESH CHARLES & 33 ST BALTIMORE MD 21218
3	PENN STATE UNIV COLLEGE OF ENGINEERING ATTN T KRAUTHAMMER R QUNEEY R GERMAN UNIVERSITY PARK PA 16802-6809
4	GENERAL RESEARCH CORP ATTN W ISBELL A CHARTERS T MENNA C PACE PO BOX 6770 SANTA BARBARA CA 93160
1	KAMAN SCIENCES CORP ATTN J WILBECK PO BOX 2486 HUNTSVILLE AL 35804-2486
2	KAMAN SCIENCES CORP ATTN N ARI S DIEHL 1500 GARDEN OF THE GODS RD COLORADO SPRINGS CO 80907
1	CONCURRENT TECH CORP ATTN T MCCABE 1450 SCALP AVE JOHNSTOWN PA 15904
2	OLIN CORP FLINCHBAUGH DIV ATTN D ROD R CAMPOU 200 E HIGH ST PO BOX 127 RED LION PA 17356

NO. OF COPIES	ORGANIZATION
2	PHYSICAL SCIENCES INC ATTN DR W REINECKE P NEBOLSINE 20 NEW ENGLAND BUS CTR ANDOVER MA 01810
1	INTERFEROMETRICS INC ATTN R LARRIVA 8150 LEESBURG PIKE STE 1400 VIENNA VA 22182-2799
1	SIMULA INC ATTN W PERCIBALLI 10016 S 51ST ST PHOENIX AZ 85044
1	ROCKWELL INTL ROCKETDYNE DIV ATTN D STEVENSON BLDG 037 PO BOX 7922 CANOGA PARK CA 91309-7922
3	OSRAM SYLVANIA INC ATTN J SPENCER J MULLENDORE S DOEPKER HAWES ST TOWANDA PA 18848
1	PARMATECH CORPORATION ATTN A BOSE 2221 PINE VIEW WAY PETALUMA CA 94954
1	H AND H SYSTEMS ATTN G HOUGH 405 WHITE ST HUNTSVILLE AL 35801
1	OLIN ORDNANCE ATTN D EDMONDS 10101 9TH ST N ST PETERSBURG FL 33716
1	BRIGGS CO ATTN J BACKOFEN 2668 PETERSBOROUGH ST HERNDON VA 22071

NO. OF COPIES	ORGANIZATION
1	EI DUPONT DE NEMOURS & CO ATTN SECURITY DIRECTOR LEGAL DEPT B SCOTT PO BOX 1635 WILMINGTON DE 19899
1	COMPUTATIONAL MECH ASSOC ATTN J ZUKAS 8600 LASALLE RD STE 614 OXFORD BLDG TOWSON MD 21204
1	DYNA EAST CORPORATION 3201 ARCH ST PHILADELPHIA PA 19104-2588
1	AEROJET ELECTRONIC SYSTEM DIVISION ATTN WARHD SYS J CARLEONE PO BOX 296 AZUSA CA 91702
1	ALLIANT TECHSYSTEMS INC PRECISION ARMAMENT SYS GROUP ATTN G JOHNSON 7225 NORTHLAND DR BROOKLYN PARK MN 55428-1516
1	MAXWELL LABORATORIES INC S CUBED DIVISION ATTN R SEDGWICK PO BOX 1620 LA JOLLA CA 92038-1620
1	TITAN CORPORATION CA RSRCH & TECH DIV ATTN M MAJERUS PO BOX 2229 PRINCETON NJ 08543-2229
2	TITAN CORP ATTN R FRANZEN D ORPHAL 5117 JOHNSON DRIVE PLEASANTON CA 94566

NO. OF COPIES	ORGANIZATION
6	ALLIANT TECHSYSTEMS INC ATTN C CANDLAND M CONRAD R JOHNSON P KILPATRICK S NEUBAUER H NORDEEN 600 SECOND ST NE HOPKINS MN 55343-8384
1	SRI INTL ATTN D CURRAN 333 RAVENWOOD AVE MENLO PARK CA 94025
1	DR R EICHELBERGER 409 W CATHRINE ST BEL AIR MD 21014-3613
1	DR W GOLDSMITH 450 GRAVATT DR BERKLEY CA 94705-1506
	ABERDEEN PROVING GROUND
11	DIR, USAMSAA ATTN: AMXSY-G AMXSY-R AMXSY-RA, K. HILTON AMXSY-LX, R. COSTABILE AMXSY-GA, W. BROOKS J. BREWER B. SIEGEL AMXSY-A, D. DRAKE AMXSY-CC, M. DECKERT AMXSY-CR, D. SMOOT
2	CDR, USAATC ATTN: STECS-AA-HT, H. GREUTER STECS-AD-A
4	CDR, USATEC ATTN: AMSTE-TA-R, L. SAUBIER AMSTE-ST-S AMSTE-TA-O AMSTE-TA-L

NO. OF COPIES	ORGANIZATION
58	DIR, USARL
	ATTN: AMSRL-MA,
	G. BISHOP
	L. JOHNSON
	AMSRL-MA-C,
	D. VIECHNICKI
	AMSRL-MA-PA,
	W. HASKELL
	AMSRL-SL-BV,
	W. BAKER
	R. SAUCIER
	R. SHNIDMAN
	AMSRL-WD,
	A. NIILER
	G. THOMSON
	AMSRL-WT,
	D. ECCLESHALL
	AMSRL-WT-PB,
	E. SCHMIDT
	AMSRL-WT-PD,
	B. BURNS
	AMSRL-WT-T,
	W. MORRISON, JR.
	T. WRIGHT
	AMSRL-WT-TA,
	S. BILYK
	W. BRUCHEY
	M. BURKINS
	M. DUFFY
	G. FILBEY
	W. GILLICH
	W. GOOCH
	T. HAVEL
	D. HACKBARTH
	M. KEELE
	E. RAPACKI
	W. ROWE
	M. ZOLTOSKI
	T. BJERKE
	R. COATES
	A. COPLAND
	W. DE ROSSET
	T. FARRAND
	F. GRACE
	ATTN: AMSRL-WT-TC,
	E. KENNEDY
	M. LAMPSON
	W. LEONARD
	L. MAGNESS
	F. MALINOSKI
	R. MUDD

NO. OF COPIES	ORGANIZATION
	DIR, USARL (CONT.)
	AMSRL-WT-TC,
	L. PRIDGEON
	D. SCHEFFLER
	G. SILSBY (5 CPS)
	R. SUMMERS
	W. WALTERS
	AMSRL-WT-TD,
	A. DIETRICH, JR.
	K. FRANK
	J. HARRISON
	M. RAFTENBERG
	G. RANDERS-PEHRSON
	S. SEGLETES
	AMSRL-WT-WB,
	L. BURKE, JR.
	W. DAMICO, JR.
	R. MCGEE
	AMSRL-WT-WC,
	J. ROCCHIO

NO. OF COPIES	ORGANIZATION
1	DR SOL BODNER TECHNION-ISRAEL INST OF TECHNOLOGY FACULTY OF MECHANICAL ENGINEERING TECHNION CITY HAIFA 32000 ISRAEL
1	DR MOSHE RAVID 4 HAQEULA STREET 45272 HOD HASHARM ISRAEL
1	DR DAN YAZIV RAFAEL PO BOX 2250 (24) HAIFA 31021 ISRAEL
1	PRINS MAURITS LABORATORIUM TNO ATTN LIBRARY PO BOX 45 2280 AA RIJSWIJK THE NETHERLANDS
4	COMMANDER RARDE FORT HALSTEAD ATTN A TATE B CLIFFORD I STONE C BRISSENDEN SEVEN OAKS KENT TN14 7BP ENGLAND UNITED KINGDOM
1	DIRECTOR MATERIALS RESEARCH LABORATORY ATTN R WOODWARD PO BOX 50 ASCOT VALE VIC 3052 AUSTRALIA
1	DIRECTOR DEFENCE RESEARCH EST VALCARTIER ATTN W ROBERTSON PO BOX 8800 COURCELLETTE QUEBEC GOA 1RO CANADA
2	ERNST-MACH-INSTITUT ATTN A STILP V HOHLER ECKERSTRASSE 4 D 7800 FREIBURG I BR GERMANY

NO. OF COPIES	ORGANIZATION
1	BOFORS WPNS SYSTEMS S-691 80 KARLSKOGA SWEDEN

INTENTIONALLY LEFT BLANK.

USER EVALUATION SHEET/CHANGE OF ADDRESS

This Laboratory undertakes a continuing effort to improve the quality of the reports it publishes. Your comments/answers to the items/questions below will aid us in our efforts.

1. ARL Report Number/Author ARL-MR-320 (Silsby) Date of Report July 1996

2. Date Report Received _____

3. Does this report satisfy a need? (Comment on purpose, related project, or other area of interest for which the report will be used.) _____

4. Specifically, how is the report being used? (Information source, design data, procedure, source of ideas, etc.) _____

5. Has the information in this report led to any quantitative savings as far as man-hours or dollars saved, operating costs avoided, or efficiencies achieved, etc? If so, please elaborate. _____

6. General Comments. What do you think should be changed to improve future reports? (Indicate changes to organization, technical content, format, etc.) _____

CURRENT ADDRESS

_____
Organization

_____
Name

_____
Street or P.O. Box No.

_____
City, State, Zip Code

7. If indicating a Change of Address or Address Correction, please provide the Current or Correct address above and the Old or Incorrect address below.

OLD ADDRESS

_____
Organization

_____
Name

_____
Street or P.O. Box No.

_____
City, State, Zip Code

(Remove this sheet, fold as indicated, tape closed, and mail.)
(DO NOT STAPLE)

DEPARTMENT OF THE ARMY

OFFICIAL BUSINESS

NO POSTAGE
NECESSARY
IF MAILED
IN THE
UNITED STATES

BUSINESS REPLY MAIL
FIRST CLASS PERMIT NO 0001,APG,MD

POSTAGE WILL BE PAID BY ADDRESSEE

DIRECTOR
U.S. ARMY RESEARCH LABORATORY
ATTN: AMSRL-WT-TC
ABERDEEN PROVING GROUND, MD 21005-5066